Energetics and Mechanism of Primary Charge Separation in Bacterial Photosynthesis. A Comparative Study on Reaction Centers of *Rhodobacter sphaeroides* and *Chloroflexus aurantiacus*

Martin Volk,*,† Gudrun Aumeier,† Thomas Langenbacher,† Reiner Feick,‡ Alexander Ogrodnik,† and Maria-Elisabeth Michel-Beyerle†

Institut für Physikalische und Theoretische Chemie, Technische Universität München, 85748 Garching, Germany, and Max-Planck-Institut für Biochemie, 82152 Martinsried, Germany

Received: August 22, 1997; In Final Form: November 13, 1997

The high efficiency of charge separation in photosynthetic reaction centers arises from the interplay of energetics, electronic couplings, and reorganization energies relevant for the fast charge separation and slow recombination processes. All these parameters can be determined unambiguously only from magnetic-field-dependent measurements of the recombination dynamics of the intermediate radical pair $P^+H_A^-$ and the lifetime of the recombination product $^3P^*$. Results obtained on Q_A-depleted reaction centers of *Chloroflexus aurantiacus* are compared with those for the well-characterized reaction centers of *Rhodobacter sphaeroides*. In contrast to *Rb. sphaeroides*, the magnetic field dependence of the triplet yield in *Cf. aurantiacus* has a pronounced resonance structure, allowing the direct determination of the exchange interaction of $P^+H_A^-$, $J = 21$ G. The recombination rate k_T is slightly larger for *Cf. aurantiacus* and shows a different temperature dependence. All these differences can be explained by the free energy of $P^+H_A^-$, found to be larger by 0.04 eV in *Cf. aurantiacus* compared to *Rb. sphaeroides*. We propose that this different energy arises largely from the different amino acid at position L104, which is glutamic acid in the case of *Rb. sphaeroides* and glutamine in the case of *Cf. aurantiacus*. The electronic couplings and the reorganization energies, on the other hand, are very similar in both reaction centers. Implications for the mechanism of primary charge separation are discussed. The pronounced nonexponential kinetics of charge separation in *Cf. aurantiacus* is explained by the energetic inhomogeneity of the primary radical pair $P^+B_A^-$.

I. Introduction

A central issue in the discussion of the mechanism of electron-transfer processes is the driving force.[1−3] The values of free-energy changes in solution normally can be derived from electrochemical measurements. In the photosynthetic reaction center (RC), however, the redox potentials of the bacteriochlorophyll (BChl) monomers and of the bacteriopheophytins (BPheo) cannot be measured electrochemically, probably due to their limited accessibility. Thus, free energy differences between the various charge-separated states in the RC have to be determined via the equilibrium constant.

Measurements of the magnetic-field-dependent recombination dynamics of the intermediate radical pair $P^+H_A^-$ and the lifetime of the recombination product $^3P^*$ allowed the determination of the equilibrium constant between $P^+H_A^-$ and $^3P^*$ and thus of the free energy of $P^+H_A^-$ in RCs of *Rhodobacter sphaeroides*.[4−6] Furthermore, a lower limit for the free energy of $P^+B_A^-$ could be given.[7] Here P denotes the primary donor, a BChl dimer, H_A is the BPheo at the active branch (i.e. the one of the two almost symmetric pigment branches of the RC along which electron transfer proceeds), and B_A is the accessory monomeric BChl located between P and H_A.[8] In addition, electronic couplings and reorganization energies were determined on the nanosecond time scale and related to the results of measurements on the picosecond time scale.[9−11]

All these parameters, especially the free energy of $P^+B_A^-$, are of high importance since the discussion of the mechanism of primary charge separation rests on them. Under debate are models in which electron transfer from P to H_A occurs either in two steps via B_A or directly to H_A with B_A enhancing the electronic interaction between P and H_A via the superexchange mechanism. After many years of controversial discussion,[2,10,12−18] recent experimental and theoretical developments[3,19−23] converged on supporting the two-step model in the case of *Rb. sphaeroides*.

It is the goal of this paper to test the universality of the energetics and mechanism of primary charge separation in bacterial RCs. This is done by a detailed comparison of the energetics and phenomenology of primary charge separation in the RC of *Rb. sphaeroides* with another RC, that of the thermophilic green bacterium *Chloroflexus aurantiacus*. The RC of *Cf. aurantiacus* is well-suited for such measurements. As for *Rb. sphaeroides R26*, no carotenoid, which inhibits the determination of the intrinsic lifetime of $^3P^*$ due to energy transfer, is present in this RC. Also, the quinone at the active branch (Q_A) can easily be removed. This permits the observation of $P^+H_A^-$ recombination dynamics without reduction of Q_A, which complicates the interpretation of the data due to the additional electron spin on Q_A and alters the energetics of the primary radical pair states. The RC of *Cf. aurantiacus* is the smallest RC isolated so far, consisting of only two protein

* Corresponding author. FAX: ++49-89-289-13026. E-mail: mvolk@zentrum.phys.chemie.tu-muenchen.de.
† Technische Universität München.
‡ Max-Planck-Institut für Biochemie.

S1089-5647(97)02743-0 CCC: $15.00
Published on Web 01/03/1998

subunits which show a significant homology to the L- and M-subunit of the RC of purple bacteria.[24] It contains 3 BPheo and 3 BChl, compared to 2 BPheo and 4 BChl in the RC of purple bacteria.[25,26] So far, no X-ray structure data are available for the RC of *Cf. aurantiacus*. The primary sequence of the two protein subunits,[24] spectroscopic evidence[27] including Stark spectroscopy,[28] and EPR measurements,[29] however, allow the conclusion that also in this RC two of the BChls form a dimer and that the pigments are arranged on two branches in analogy with the RC of purple bacteria.

However, there are some prominent differences in the primary sequence of the RC of *Cf. aurantiacus*[24] compared to the RC of purple bacteria[8] which might be relevant for the mechanism of charge separation and the extent of its unidirectionality: (i) *Histidine*^{M182} in the *Rb. sphaeroides* RC is replaced by leucine in the RC of *Cf. aurantiacus*, suggesting that it is the BChl at the inactive branch that is replaced by a BPheo. Despite this replacement, charge separation proceeds exclusively via the A-branch in *Cf. aurantiacus*[30,31] and has a quantum yield near unity,[32] in analogy with charge separation in *Rb. sphaeroides*. (ii) *Glutamic acid*^{L104}, which is hydrogen-bonded to the keto oxygen of ring V of H_A,[33] is replaced by glutamine in *Cf. aurantiacus*. The protonated glutamic acid was predicted to significantly stabilize the state $P^+H_A^-$,[34,35] so that its replacement by glutamine should lead to an increased energy of this state. (iii) *Tyrosine*^{M210}, which is in van der Waals distance to P, B_A, and H_A, is replaced by nonpolar leucine in *Cf. aurantiacus*. From electrostatic calculations[35] and experimental results on site-directed mutants of *Rb. sphaeroides*[36−38] this replacement is expected to affect the energy of $P^+B_A^-$, which is the deciding factor for the mechanism of primary charge separation.

In RCs of *Cf. aurantiacus* primary charge separation from P to H_A proceeds with an average time constant of about 7 ps at room temperature.[39] Fluorescence upconversion measurements actually show a biexponential decay of $^1P^*$ with time constants of 3 and 9 ps.[40] At lower temperatures a pronounced biexponential behavior was observed with time constants of about 2−3 and 20−30 ps below 100 K with similar amplitudes.[39,41,42] These values yield an average time constant of 11 ps, thus showing a slight activation of the charge separation process. Notably smaller deviations of primary charge separation from exponentiality were reported for *Rb. sphaeroides*.[40,43] Here, charge separation from P to H_A occurs with a time constant of 3−4 ps at room temperature,[17,19,44,45] decreasing to 1−2 ps below 100 K,[20,45,46] revealing an inverted temperature dependence.

The pronounced nonexponentiality and the slight activation of primary charge separation in RCs of *Cf. aurantiacus* might have significant implications for the mechanism of charge separation. For a detailed discussion, the relevant parameters, including the energetics of the charge-separated states, have to be known. In the following, we report measurements of the recombination dynamics of $P^+H_A^-$ which allow the determination of these parameters. Differences between the results for the two RCs will be explicitly related to differences in their amino acid composition. We will conclude that, as for *Rb. sphaeroides*, charge separation in *Cf. aurantiacus* is governed by the two-step mechanism, at least at physiological temperatures. The deviations of charge separation from monoexponentiality in both RCs can be explained by the energetic inhomogeneity of radical pair states.[47] They are more pronounced in the RC of *Cf. aurantiacus* because of a smaller free energy gap for primary charge separation. A preliminary report of these results has been given in ref 38.

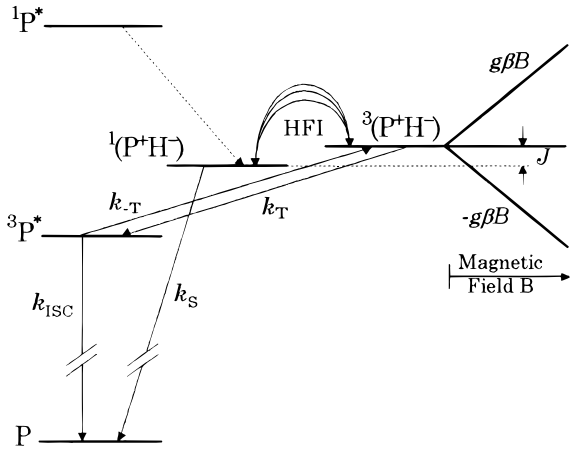

Figure 1. Kinetic scheme for the recombination of $P^+H_A^-$ in Q_A-depleted RCs. The energetic splitting of $^1(P^+H_A^-)$ and $^3(P^+H_A^-)$ due to exchange interaction (J) and Zeeman interaction ($\pm g\beta B$) are not to scale.

II. Methodology: Recombination Dynamics of the Radical Pair $P^+H_A^-$

In Q_A-depleted or Q_A-reduced RCs recombination of the radical pair $P^+H_A^-$ proceeds on the nanosecond time scale to the ground state P with the rate k_S or after hyperfine (HFI)-induced singlet−triplet−mixing (S−T mixing) to the triplet state $^3P^*$ with the (faster) rate k_T, Figure 1.[5,9,48−57] S−T mixing is hindered by the energetic splitting of the singlet and triplet radical pair states (exchange interaction J). Therefore, in an external magnetic field the maximum triplet yield Φ_T is found for the field $B_{max} \approx J/g\beta$ (here g denotes the electron g-factor and β Bohr's magneton), for which Zeeman interaction results in one of the triplet states being isoenergetic with the singlet state. On increasing the magnetic field above B_{max}, a steady decrease of Φ_T, accompanied by a concomitant increase of the radical pair lifetime τ_{RP}, is observed, saturating above 500 G (magnetic field dependence of the reaction yield, MARY). The half-width ΔB of the MARY spectrum around resonance is determined by inhomogeneous broadening due to hyperfine interaction and homogeneous broadening reflecting the lifetime of the radical pair levels, with the latter constituting the dominant contribution.[54−56] The singlet recombination rate k_S can be directly obtained from τ_{RP} and Φ_T[5,55] and cannot account for the width. Thus, ΔB is a measure for k_T.[9] For Q_A-depleted RCs of *Rb. sphaeroides* a value of 5×10^8 s^{-1} was found for k_T, almost independent of the temperature,[9,58−60] while k_S decreases from 5×10^7 s^{-1} at room temperature to 1.5×10^7 s^{-1} at 90 K.[5] For unmodified RCs of *Rb. sphaeroides*, the exchange interaction J is found to be small ($J/g\beta \approx 10$ G) compared to ΔB (∼50 G),[9,51,53,58,60−62] so that no clear resonance in the MARY spectrum is observed. Recently, a clear resonance near 25 G was observed in Q_A-depleted RCs of *Rb. sphaeroides*, in which *Tyrosine*^{M210} was replaced by tryptophan.[63]

III. Time-Resolved Absorbance Measurements in External Magnetic Fields

Materials. RCs of *Cf. aurantiacus* were prepared according to ref 64. For the extraction of Q_A, RCs were extensively washed with 1 L of Tris-Cl buffer (20 mM, pH 8.0) containing 0.2% Triton X-100. This concentration of Triton X-100 is sufficient to remove Q_A in more than 99% of the *Cf. aurantiacus*

TABLE 1: Temperature-Dependent Results for Q_A-Depleted RCs of *Cf. aurantiacus*[a]

		T [K]										
		75	90	120	150	180	200	230	250	270	290	310
τ_{RP} [ns]	0 G	24.2	23.8	24.7	23.1	22.2	21.0	17.2	14.6	12.9	11.4	11.5
	23 G							16.2	13.5	12.1	10.7	10.6
	700 G	32.6	32.5	33.8	32.7	32.1	29.7	22.4	19.1	16.2	14.1	14.5
Φ_T	0 G	0.49	0.50	0.53	0.54	0.53	0.50	0.42	0.36	0.31	0.28	0.32
	23 G						0.26	0.44	0.39	0.34	0.30	0.34
	700 G	0.26	0.26	0.27	0.28	0.28		0.21	0.17	0.14	0.14	0.15
B_{res} [G]								22	22	21	22	20
$B_{1/2}$ [G]		124	115	104	95	90	83	67	62	62	55	53
ΔB [G]		103	94	83	74	69	62	46	41	41	34	32
k_S [10^7 s^{-1}]		2.4	2.4	2.3	2.3	2.3	2.5	3.6	4.3	5.2	6.0	5.8
τ_3 [μs]	0 G	103	103	101	101	100	102	96	93	87	80	74
	700 G	102	102	101	102	101	103	98	99	92	87	83
ΔG_T [eV]								0.186	0.182	0.198	0.196	0.206

[a] τ_{RP} lifetime of $P^+H_A^-$ ($\pm$1 ns); Φ_T recombination yield of $^3P^*$ ($\pm$0.01); B_{res} resonance magnetic field of MARY spectrum ($\pm$1 G); $B_{1/2}$ magnetic field at which half of the full magnetic field modulation of Φ_T is observed ($\pm$1 G); ΔB width of the MARY spectrum (hwhm) ($\pm$1 G); k_S singlet recombination rate ($\pm 0.2 \times 10^7$ s^{-1}), determined with eq 3; τ_3 lifetime of $^3P^*$ ($\pm$2 μs); ΔG_T free-energy gap between $P^+H_A^-$ and $^3P^*$ ($\pm$0.01 eV), determined with eq 5.

RCs, while much higher concentrations of detergent and the addition of *o*-phenanthroline are necessary to obtain a similar result for RCs of *Rb. sphaeroides*.[65] The loose binding of Q_A in RCs of *Cf. aurantiacus* might be due to the absence of the H protein subunit.[24] Elution of the RCs was accomplished with 100 mM NaCl in 20 mM Tris-Cl (pH 8.0)/0.2% Triton X-100. After dialysis the RCs were concentrated to about 120 μM in 20 mM Tris (pH 8.0)/0.1% Triton X-100. The preparation of Q_A-depleted RCs of *Rb. sphaeroides R26* has been described in ref 5, yielding typically 160 μM RCs in Tris buffer (20 mM, pH 8.0)/0.1% Nonidet P40. After preparation, the RC samples were stored in liquid nitrogen. Immediately before the measurement they were diluted with the appropriate buffer solution and glycerol to yield samples with 60% glycerol and an absorbance of about 0.5 in the Q_y-band of P around 865 nm (optical pathlength 2 mm).

Experimental Details. RCs were excited at 600 nm with a Nd:YAG-laser-pumped dye laser (pulse width 1.8 ns, 8 Hz) with an energy density of about 0.5 mJ/cm^2, corresponding to a yield of about 20% excited RCs. Absorbance changes in the maximum of the Q_y-transition of P around 865 nm were probed with a N_2-laser-pumped dye laser (pulse width 1.5 ns). For most measurements, the polarizations of pump and probe light were adjusted to be parallel. The delay time between excitation and probing pulse was adjusted electronically between 0 ns and 10 ms in steps of 1 ns (programmable delay generator Le Croy 4222) and monitored with a time-to-digital converter (Le Croy 4202, resolution 150 ps) to correct for laser trigger jitter and drifts. A magnetic field of up to 700 G was applied by a pair of Helmholtz coils. More experimental details have been described in ref 65.

The fraction of RCs still containing residual Q_A was determined and corrected for by measuring the contribution of $P^+Q_A^-$ to the P absorbance bleaching. Since in RCs of *Rb. sphaeroides* and *Cf. aurantiacus* $P^+Q_A^-$ is formed within a few 100 ps[30,66] and recombines on the 100-ms time scale,[25,67] its contribution can easily be discriminated from the nano- and microsecond components of Q_A-depleted RCs.[65] Within an accuracy of better than 1%, no Q_A-containing RCs could be detected in the case of *Cf. aurantiacus*, while about 5% of the RCs of *Rb. sphaeroides* contained Q_A. All data shown and discussed here have been corrected by subtracting the contribution of $P^+Q_A^-$ from the measured signal.

To ensure that freezing or thawing did not damage the RCs, cyclic measurements were performed. In all cases, the first and last result of a measuring cycle were identical within experimental accuracy.

Results. The recombination dynamics of $P^+H_A^-$ in Q_A-depleted RCs of *Cf. aurantiacus* was investigated in the temperature range 90−310 K. Analogous measurements had been performed previously in our laboratory on RCs of *Rb. sphaeroides* using an experimental setup with an optical delay between the exciting and probing pulses.[5] In that case, the delay time was limited to a maximum value of 92 ns. Measurements on *Rb. sphaeroides* at 90 and 290 K were repeated in the present setup with electronic delay and extended to the microsecond time scale. The results on the nanosecond time scale obtained in the two measuring modes essentially were the same; see Table 2.

Kinetics. Figure 2 shows the time-dependent recovery of the P ground-state absorbance in RCs of *Cf. aurantiacus* at 90 K. Parallel to the recombination of $P^+H_A^-$ to the singlet ground state the absorbance recovers on the nanosecond time scale. The persisting bleaching of P at longer delay times indicates the partial formation of $^3P^*$. This residual bleaching decays with a time constant of about 100 μs. In a magnetic field of >500 G the recombination of $P^+H_A^-$ is slowed down significantly and yields less triplets due to the inhibition of S−T mixing to two of the three triplet sublevels by Zeeman splitting.

In a first approximation, the data can be described by

$$\Delta A = \Delta A_0[(1 - \Phi_T)e^{-t/\tau_{RP}} + \Phi_T e^{-t/\tau_3}] \qquad (1)$$

with ΔA_0 denoting the initial bleaching of the P absorbance at $t = 0$, τ_{RP} the lifetime of the radical pair $P^+H_A^-$, τ_3 the lifetime of $^3P^*$, and Φ_T the triplet recombination yield.[68]

For fitting, data at delay times shorter than 5 ns were not considered because of the slight lag in the radical pair decay arising from coherent S−T mixing.[5] Nevertheless, a fit of the data at delay times between 5 and 200 ns shows significant deviations of $P^+H_A^-$ recombination from monoexponentiality; see the residuals in Figure 2. These deviations were observed for *Cf. aurantiacus* as well as for *Rb. sphaeroides* and are due to the inherent heterogeneity of the RCs with respect to the conformation of the nuclear spins driving S−T mixing.[38,42,70] The energetic inhomogeneity of $P^+H_A^-$,[47] on the other hand, which also could contribute to the nonexponentiality of radical pair recombination, can be shown to be only of minor significance.[71] The deviations of radical pair recombination from monoexponentiality complicate the analysis of the data

TABLE 2: Temperature-Dependent Results for Q_A-depleted RCs of *Rb. sphaeroides*, Determined in Two Setups Using an Optical or an Electronic Delay between Exciting and Probing Laser Pulse[a]

		electronic delay		optical delay							
T [K]		90	290	90	120	150	185	230	250	270	290
τ_{RP} [ns]	0 G	22.7	13.5	23.7	21.3	19.5	19.3	17.5	15.6	13.8	13.3
	700 G	38.4	19.1	39.8	32.4	27.6	25.5	23.0	19.2	17.4	16.4
Φ_T	0 G	0.63	0.32	0.71	0.61	0.52	0.45	0.39	0.34	0.31	0.30
	700 G	0.39	0.16	0.50	0.45	0.38	0.34	0.26	0.23	0.20	0.18
$B_{1/2}$ [G]		55	38	55	51	52	51	46	45	43	42
ΔB [G]		45	28	45	41	42	41	36	35	33	32
k_S [10^7 s^{-1}]		1.6	4.0	1.3	1.6	1.9	2.2	3.0	3.8	4.2	4.7
τ_3 [μs]	0 G	135	54.4	135[b]			116[b]	94[b]	78[b]	65[b]	51[b]
	700 G	133	71.8	135[b]			119[b]	101[b]	89[b]	76[b]	68[b]
ΔG_T [eV]			0.155				0.131	0.148	0.146	0.152	0.155

[a] Abbreviations and error margins are the same as in Table 1. The measurements using the setup with optical delay have been published before.[5] The slightly different values for τ_{RP}, Φ_T and k_S given here are due to the consideration of data after 5 ns only, while in ref 5 data after 3 ns were included. Furthermore, k_S here was determined using an improved method, eq 3, which is insensitive to the absolute value of Φ_T (see text). [b] Data from ref 4 (τ_3 at 0 and 500 G).

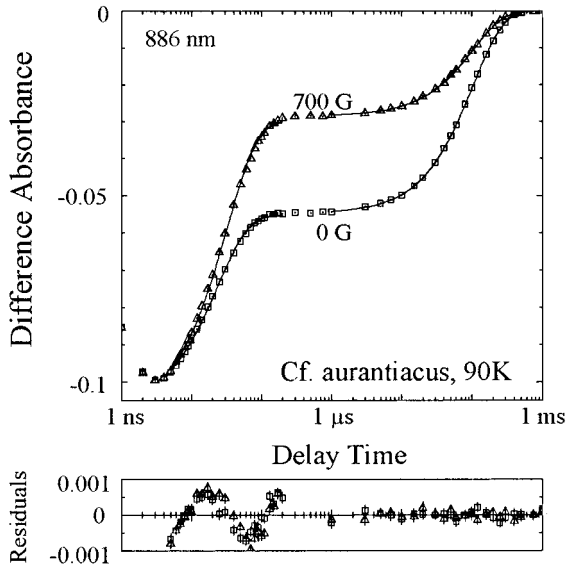

Figure 2. Time-dependent recovery of the P absorbance bleaching at 886 nm in Q_A-depleted RCs of *Cf. aurantiacus* at 90 K, 0 G (□) and 700 G (△). Solid lines are independent monoexponential fits of the data at delay times 5−200 ns and 1−500 μs, respectively, the results of which are given in Table 1. Also shown are the residuals of the fits.

on the nanosecond time scale. The values for τ_{RP} in Tables 1 and 2 are the results of monoexponential fits of the data at delay times between 5 and 200 ns, whereas the values of Φ_T were obtained using biexponential fits, which yield the most reliable results.[72]

For both RCs, the decay of ^{3}P* at 90 K could be well fitted to a single exponential; see the residuals in Figure 2. Above 250 K rotational depolarization of the RCs in the viscous buffer/glycerol medium occurs on the microsecond time scale. This distorts the observed recovery of the P ground-state absorbance when measuring with parallel polarization of probing and excitation light. Here, biexponential fits were employed, yielding the ^{3}P* lifetime, τ_3, and a faster time constant, which is governed by rotational depolarization. However, even these biexponential fits of the P absorbance recovery on the microsecond time scale at temperatures above 250 K yielded residuals several times larger than the error of the measurement ($\Delta\Delta A \approx 2 \times 10^{-4}$), indicating a distribution of time constants for the decay of ^{3}P*. This issue will be discussed in more detail below.

Tables 1 and 2 summarize the temperature-dependent values of τ_{RP}, Φ_T, and τ_3 for RCs of *Cf. aurantiacus* and *Rb. sphaeroides*. For each temperature, the probing wavelength was adjusted to the maximum of the P absorbance bleaching, shifting from 886 nm at 90 K to 862 nm at 290 K for *Cf. aurantiacus*. The absolute values as well as the temperature dependence of τ_{RP}, Φ_T, and τ_3 are similar in *Rb. sphaeroides* and *Cf. aurantiacus*. In both cases the radical pair lifetime and the triplet yield increase with decreasing temperature. The dynamics of $P^+H_A^-$ recombination as well as the yield of ^{3}P* significantly depend on the external magnetic field. For *Cf. aurantiacus* at temperatures above 230 K the dynamics also were measured at a magnetic field of 23 G, that is, close to the resonance field of MARY spectra. In parallel to the observation of the maximum triplet yield, recombination is observed to proceed fastest at this magnetic field.

MARY Spectra. The magnetic field dependence of the triplet yield (MARY spectrum) between 0 and 700 G was measured at a delay time of 200 ns (92 ns in the setup with optical delay), that is, after completion of radical pair recombination. Figure 3 shows MARY spectra for *Cf. aurantiacus* at various temperatures. Above 230 K a pronounced resonance structure was observed, allowing the direct determination of the exchange interaction, J, of $P^+H_A^-$. At lower temperatures no such resonance could be resolved due to the increasing widths of the MARY spectra. Similar spectra without resonances were obtained for *Rb. sphaeroides* for most temperatures, with the exception of 230 K, where a weak resonance near 10 G was found (data not shown). For the spectra without resonance structure, the "true" width ΔB (hwhm) was estimated by subtracting the value of J (∼10 G for *Rb. sphaeroides* and ∼21 G for *Cf. aurantiacus*, both essentially temperature-independent; see below) from the value $B_{1/2}$ of the magnetic field at which half of the maximum magnetic field modulation of Φ_T was observed. ΔB was found to increase from 34 G at 290 K to 94 G at 90 K in the case of *Cf. aurantiacus*, while it is almost temperature-independent in the case of *Rb. sphaeroides*.

The sets of parameters presented in Tables 1 and 2 have been measured with highest accuracy on a single sample of RCs of *Cf. aurantiacus* and *Rb. sphaeroides*, respectively. For *Cf. aurantiacus* this is the first time these parameters were determined. For *Rb. sphaeroides* the values given here agree well with previously published values.[4−6,9,48−53,57]

IV. Deduction of the Recombination Parameters

For RCs of *Rb. sphaeroides* it has been shown that the triplet recombination rate k_T is considerably larger than the singlet recombination rate k_S.[5,51,52,57,58,60] This conclusion follows directly from the observed increase of τ_{RP} in an external

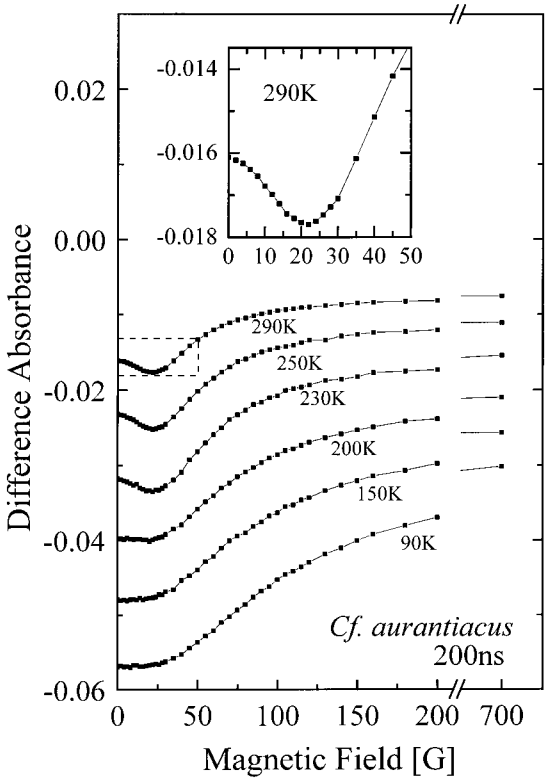

Figure 3. Magnetic field dependence of the Q_y-absorbance bleaching of P in Q_A-depleted RCs of *Cf. aurantiacus* at different temperatures, 200 ns after excitation (MARY spectra). Inset: enlargement of MARY spectrum at 290 K.

magnetic field, which increases the yield of recombination via the (slower) singlet channel. Also, the lifetime broadening, as reflected in the width ΔB of the MARY spectrum, implies the recombination rate of at least one of the states $^1(P^+H_A^-)$ or $^3(P^+H_A^-)$ to be larger than 5×10^8 s^{-1}. On the other hand, τ_{RP}, being on the order of 10 ns, is longer than expected from such a rate, reflecting slow recombination in the initially formed $^1(P^+H_A^-)$ state. S−T mixing occurs on a similar time scale, thus constituting a bottleneck for the faster recombination via the triplet channel. The same features are observed for *Cf. aurantiacus* and thus allow the same conclusion.

The Singlet Recombination Rate k_S. The radical pair lifetime τ_{RP} is given by[55]

$$\tau_{RP} = \frac{1 - \Phi_T}{k_S} + \frac{\Phi_T}{k_T} \qquad (2)$$

Application of eq 2 to the radical pair lifetimes measured at zero magnetic field and in a magnetic field B yields

$$k_S = \frac{\Phi_T(0)/\Phi_T(B) - 1}{\tau_{RP}(B)\Phi_T(0)/\Phi_T(B) - \tau_{RP}(0)} \qquad (3)$$

The values of k_S obtained from eq 3 for *Cf. aurantiacus* and *Rb. sphaeroides* are included in Tables 1 and 2. They were found to be very similar. For both RCs the singlet recombination rate only weakly depends on the temperature, being reduced by a factor of 3 when lowering the temperature from 290 to 90 K.

It has to be emphasized that the determination of k_S from eq 3 rests on the magnetic field modulation of Φ_T and is independent of the absolute value of Φ_T. Therefore, systematic errors of Φ_T from the residual absorption of H_A^- at the probing wavelength or by fast equilibration of $^3P^*$ with another state, as proposed below, do not distort the value of k_S.

Simulations of the Spin-Dependent Recombination Dynamics of $P^+H_A^-$. The determination of the rate k_T and the exchange interaction J is not possible without an explicit numerical simulation of the spin-dependent recombination dynamics of $P^+H_A^-$. This involves the solution of the stochastic Liouville equation using the appropriate spin Hamilton operator.[55,56,73] In practice, the large number of the nuclear spins at P and H_A cannot be considered explicitly, but one may resort to approximative methods, such as the one-proton model[55] or the method of equivalence factoring.[51,74] Here we have employed a semiclassical model, which describes the manifold of possible configurations of the nuclear spins interacting with the electron spin by a distribution of local magnetic fields.[75] The width of this distribution is given by the inhomogeneous broadening of the EPR line of the respective radical due to HFI. The line widths were found to be 9.5 G for P^+ and 13 G for H_A^- in RCs of *Rb. sphaeroides*[76,77] and 9.8 G for P^+ in RCs of *Cf. aurantiacus*.[29] The value for H_A^- in *Cf. aurantiacus* is assumed to be identical to that found for *Rb. sphaeroides*. The dipole interaction between the two radical electron spins has a value of 5.5 G and can be neglected.[78] Similarly, the difference of the g-factors of P^+ and H_A^- can be neglected for the magnetic fields employed here.[49]

In principle, the rates k_S and k_T and the exchange interaction J can be determined by fitting the experimental results to the time dependence of recombination of $P^+H_A^-$ and the magnetic field dependence of the triplet yield calculated in the semiclassical model with k_S, k_T, and J as free parameters of the fit. For *Cf. aurantiacus* at 90 and 290 K and for *Rb. sphaeroides* at low temperatures such fits indeed yield a good correspondence between theoretical data and experimental results. For *Rb. sphaeroides* at room temperature, however, it was not possible to match the complete set of experimental results with theoretical data. Here, a good agreement between experimental and theoretical data only can be found under the assumption that the yield of recombination via the triplet channel is larger by about 40−50% than the concentration of $^3P^*$ actually observed. This discrepancy is attributed to a fast equilibration of $^3P^*$ with the triplet state of BChl at the B-branch (B_B), which will be discussed in section VI.

Extensive numerical simulations have shown that it is sufficient to consider only the shape of the MARY spectrum and the relative modulation of Φ_T by the magnetic field for the fit of the experimental results. Therefore, we chose to ignore the observed concentration of $^3P^*$ when fitting the *Rb. sphaeroides* results at room temperature, since the observed yield does not reflect the total yield of recombination to $^3P^*$. For *Rb. sphaeroides* at low temperatures as well as for *Cf. aurantiacus*, on the other hand, essentially the same results were obtained when using the yield of $^3P^*$ (Φ_T) as the absolute yield of recombination via the triplet channel as when using only relative values.

The Triplet Recombination Rate k_T. A direct determination of k_T from τ_{RP} and Φ_T, comparable to the determination of k_S from eq 3, is not possible since the contribution of the second term in eq 2 is only small, and therefore, k_T has no significant direct contribution to the value of τ_{RP}.

Instead, the width ΔB of the MARY spectrum is a well accessible measure for k_T. Values of k_T calculated under the assumption of ΔB being the homogeneous width due to k_T are shown in Figure 4. However, there are other factors such as HFI, dipole interaction, and lifetime broadening due to k_S contributing to the MARY width. A more quantitative deter-

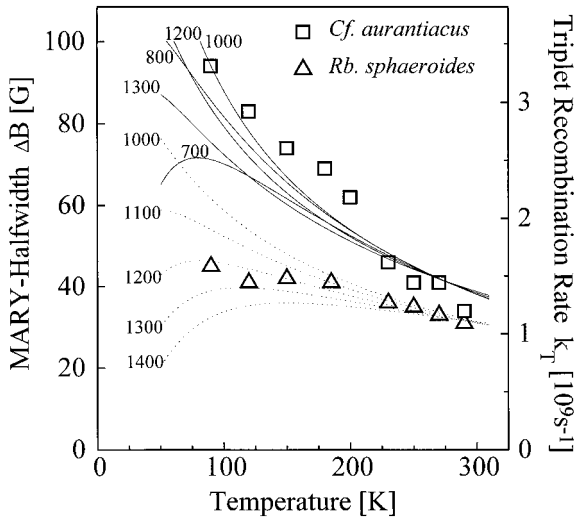

Figure 4. Temperature dependence of the MARY width ΔB (left ordinate) for Q_A-depleted RCs of *Cf. aurantiacus* (□) and *Rb. sphaeroides* (△). The size of the symbols corresponds to the error of the measurement. On the right-hand ordinate ΔB is converted to the triplet recombination rate k_T under the assumption of lifetime broadening due to k_T being dominant ($k_T = (4\pi/h)g\beta\Delta B$). The solid and dotted lines are simulations of k_T for *Cf. aurantiacus* and *Rb. sphaeroides*, respectively, using eq 7. For these simulations, temperature dependent values of $\Delta G_T = \Delta H_T - T\Delta S_T$ were calculated from the values of ΔH_T and ΔS_T given in the text, the values used for λ_T are indicated in the figure (in [cm^{-1}]), and the values of V_T were chosen to scale the curves to the same value at high temperatures for all simulations.

mination of k_T was obtained from fits of the experimental results to spectra calculated with the semiclassical model as described above. These yielded values of $k_T \approx 0.8-0.95$ ns^{-1} in the case of *Rb. sphaeroides*, almost independent of the temperature. For *Cf. aurantiacus* a value of $0.9-1$ ns^{-1} was obtained at 290 K, increasing to $2-2.5$ ns^{-1} at 90 K. These values are only slightly smaller than those calculated directly from ΔB.

The values of k_T obtained here are larger than values determined from RYDMR (reaction yield detected magnetic resonance) measurements in external magnetic and microwave fields. These yielded temperature-independent values of $0.3-0.5$ ns^{-1} for *Rb. sphaeroides*[58,60,79] and values of $0.6-0.9$ ns^{-1} at 290 K and $1.1-1.6$ ns^{-1} at 200 K for *Cf. aurantiacus*.[58,80] All these values were found to depend on the employed microwave power. The different results obtained from MARY and RYDMR spectra can be explained in light of the recently reported energetic inhomogeneity of $P^+H_A^-$, which was shown to result in a heterogeneity of the RCs with respect to the value of k_T.[47] The amplitude of MARY spectra is not very sensitive to the value of k_T.[81] Consequently, a MARY spectrum which is a composite of spectra for different values of k_T will have a width corresponding approximately to the average value of k_T. In contrast, the amplitude of RYDMR signals decreases rapidly with increasing k_T, particularly at low microwave powers.[82] Therefore, the overall RYDMR signal from a sample which is inhomogeneous with respect to k_T will not be sensitive to contributions from RCs with larger k_T, and values of k_T derived from such measurements will be smaller than the average value of k_T.

The lifetime of $P^+H_A^-$ in very high magnetic fields, leading to fast Δg-induced S−T mixing, represents an alternative approach to k_T. A value of 0.4 ns^{-1} was determined for *Rb. sphaeroides* from time-resolved fluorescence measurements,[59] again significantly smaller than the value found here. However, the limited time resolution of ref 59 and the presence of other fast fluorescence components excluded the discrimination of contributions resulting from RCs with large k_T, that is, small radical pair lifetimes, thus yielding a value for k_T smaller than the average value determined from MARY spectra.

The Exchange Interaction *J*. For RCs of *Cf. aurantiacus* a resonance was observed in the MARY spectra above 230 K with a maximum near 22 G, indicating that one of the triplet levels is degenerate with the singlet level at this field. However, theoretical simulations show that in the case of a small exchange interaction ($J/g\beta < \Delta B$) the maximum triplet yield is not observed exactly at $B = J/g\beta$. In this case, the exact value of J has to be obtained from a numerical fit of the MARY spectrum to spectra calculated with the semiclassical model described above. For *Cf. aurantiacus* such fits yielded a value for $J/g\beta$ of 21 G at 310 K, increasing to 25 G at 230 K. RYDMR measurements gave similar results.[58,80] Below 200 K no resonance structure was observed; therefore, no precise determination of J was possible from the MARY spectra. We want to point out that the values given here refer to the absolute values of the exchange interaction, since MARY spectra are sensitive only to the absolute value and not to the sign of J. In fact, the relative energetics of $^1P^*$, $P^+H_A^-$, and $^3P^*$ suggest the sign of J to be negative in the case of *Cf. aurantiacus*; that is, $^3(P^+H_A^-)$ is higher in energy than $^1(P^+H_A^-)$; see below.

No significant resonance structure was observed in the MARY spectra of *Rb. sphaeroides*, except for a weak resonance near 10 G at 230 K. From the shape of the spectra an upper limit of J in the range 10−15 G can be deduced. This is in good agreement with the results of RYDMR and EPR measurements, yielding a value of 10 ± 2 G for J in the temperature range from 95 to 290 K.[48,53,58,60,61] Recently, the direct observation of the EPR spectrum of $P^+H_A^-$ was reported.[62] Preliminary simulations of this spectrum yielded a value of $J = -9$ G for *Rb. sphaeroides*.

V. The Energetics of the Radical Pairs $P^+H_A^-$ and $P^+B_A^-$

The Determination of $\Delta G_T = \Delta G(P^+H_A^- - {}^3P^*)$ − Method. The triplet state $^3P^*$ decays to the ground state via intersystem crossing with the rate k_{ISC} and via thermal repopulation of $^3(P^+H_A^-)$ with the equilibrium constant k_{-T}/k_T, followed by triplet−singlet mixing (T−S mixing) and recombination to the ground state, Figure 1. This additional channel leads to an acceleration and magnetic field dependence of the decay of $^3P^*$ at higher temperatures;[4,5] see Tables 1 and 2. A thorough treatment[4] yields for the overall decay rate of $^3P^*$

$$1/\tau_3(B) = k_3(B) = k_{ISC} + \frac{1}{3}k_S\Phi_T(B)\frac{k_{-T}}{k_T} = k_{ISC} + \frac{1}{3}k_S\Phi_T(B)e^{-\Delta G_T/k_BT} \quad (4)$$

where Φ_T is the triplet yield of $P^+H_A^-$ recombination, $\Delta G_T = \Delta G(P^+H_A^- - {}^3P^*)$, k_B is the Boltzmann constant, and T is the temperature. The determination of τ_3 at two different magnetic fields (e.g. 0 G and $B = 700$ G) allows one to separate the two contributions to the triplet decay and solve for ΔG_T:[5]

$$\Delta G_T = -k_BT\ln\left(\frac{k_{-T}}{k_T}\right) = -k_BT\ln\left(\frac{1/\tau_3(0) - 1/\tau_3(B)}{\Phi_T(0) - \Phi_T(B)}\frac{3}{k_S}\right) \quad (5)$$

For eq 4, it was assumed that T−S mixing after repopulation of $^3(P^+H_A^-)$ is governed by the same interactions as S−T mixing leading to the formation of $^3P^*$. This assumption is

valid only if the formation of ^{3}P* does not lead to a preferential selection of RCs. However, S−T mixing does select certain RCs distinguished (i) by their orientation in the magnetic field due to anisotropic interactions and (ii) by their nuclear spin configuration.

Orientational selection (i) can be ignored at higher temperatures, where fast rotational depolarization occurs even in glycerol/buffer. For the magnetic fields used here, where the anisotropic Δg-tensor (the difference between the g-tensors of P^+ and H_A^-) does not lead to significant S−T mixing,[49] orientational selection can be ignored even at lower temperatures, since the dipole interaction between the radical electrons is small,[78] as is the effect of the anisotropy of the hyperfine interaction.[83,84]

At low magnetic fields one has to explicitly consider the nonequilibrium distribution of the nuclear spin configuration (ii) in ^{3}P* (nuclear spin polarization, NSP). It initially arises from the preferential formation of ^{3}P* in RCs with large effective HFI due to a parallel alignment of nuclear spins. In contrast, for RCs in which the HFIs with different nuclear spins partly cancel, the radical pair will recombine predominantly to the singlet ground state. If nuclear spin lattice relaxation (NSLR) is fast compared to the decay of ^{3}P*, the nuclear spin configurations are completely random and, thus, are the same for S−T and T−S mixing. In this case, eq 4 is correct. On the other hand, if NSLR is comparable to or slower than the decay of ^{3}P*, T−S mixing on the *average* will be faster than S−T mixing. Thus, the decay rate of ^{3}P* will be larger than expected from eq 4. The effects of NSP are negligible in high magnetic fields, where S−T and T−S mixing mostly are driven by the difference in the g-values for the two radicals. The comparison of low-field results with those obtained at high magnetic fields shows a small effect of NSP on τ_3 at 0 G (of ~7%),[6] indicating that NSLR does not completely randomize the nuclear spin orientations before the decay of ^{3}P*. On the other hand, the observation of a photochemically induced dynamic nuclear polarization signal in NMR spectra of RCs of *Rb. sphaeroides* indicates some NSLR to occur within the lifetime of ^{3}P*.[85] Since we have no means of quantitatively determining the degree of NSP and NSLR, there is no feasible method to take NSP into account explicitly for the determination of ΔG_T from our results. However, the numerical simulations described in the Appendix show that neglecting NSP does not significantly distort the value of ΔG_T. A maximum overestimation of ΔG_T by less than 0.015 eV is expected even if no NSLR occurred at all during the lifetime of ^{3}P*. Consequently, we will use eq 5 to determine ΔG_T from our data.

In principle, the decay of ^{3}P* also could proceed via the alternative B-branch, if $P^+H_B^-$ was more favorable in energy than $P^+H_A^-$. However, it has been shown explicitly for RCs of *Rb. sphaeroides* that the magnetic field dependence of τ_3 corresponds to that of Φ_T,[4] as expected from eq 4. If the decay of ^{3}P* proceeded via T−S mixing in $P^+H_B^-$, this correspondence would be purely coincidental. Therefore, we conclude that charge separation from ^{3}P* indeed proceeds to the A-branch in RCs of *Rb. sphaeroides*. Measurements on RCs of *Cf. aurantiacus* at 290 K yielded the same correspondence of the magnetic field dependence of τ_3 and Φ_T (data not shown), confirming that also in *Cf. aurantiacus* ^{3}P* partly decays via $P^+H_A^-$ at higher temperatures.

The Free Energy of $P^+H_A^-$. Temperature-dependent values of ΔG_T obtained from our data with eq 5 are given in Tables 1 (*Cf. aurantiacus*) and 2 (*Rb. sphaeroides*). The value of ΔG_T for RCs of *Cf. aurantiacus*, determined here for the first time, is found to be larger than that in RCs of *Rb. sphaeroides* by about 0.04 eV, independent of the temperature. The values for *Rb. sphaeroides* are slightly different from our previously published values[5] because of the improved method for determining k_S, not relying on the absolute value of Φ_T. A value for ΔG_T of 0.170 ± 0.004 eV has been reported for RCs of *Rb. sphaeroides* at room temperature from measurements in high magnetic fields,[6] which is slightly larger than the value of 0.155 ± 0.01 eV given here. This difference partly arises from the different value of k_S used in ref 6 and partly from the uncertainty of measurement. We want to emphasize that the neglect of NSP leads to an overestimation of ΔG_T and thus cannot be responsible for this difference.

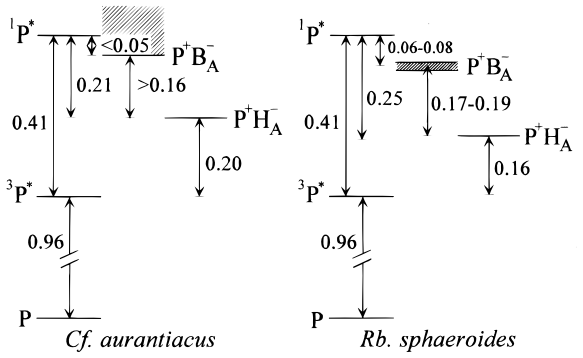

Figure 5. Average free-energy gaps between the different states involved in primary charge separation and recombination (in eV, at room temperature) for RCs of *Rb. sphaeroides* and *Cf. aurantiacus*. For details see text.

For both RCs, ΔG_T is almost temperature-independent for the accessible range between 200 and 300 K. Provided that the enthalpy difference ΔH_T and the entropy difference ΔS_T between $P^+H_A^-$ and ^{3}P* are temperature-independent, values of $\Delta H_T = 0.13 \pm 0.05$ eV and $\Delta S_T = -(2.5 \pm 1) \times 10^{-4}$ eV/K for *Cf. aurantiacus* and $\Delta H_T = 0.10 \pm 0.03$ eV and $\Delta S_T = -(2 \pm 1) \times 10^{-4}$ eV/K for *Rb. sphaeroides* can be determined from a linear fit of the temperature dependence of ΔG_T. In ref 6 a larger value of ΔH_T in RCs of *Rb. sphaeroides* of 0.18 eV was reported. However, for this determination, Φ_T and k_S were assumed to be independent of T, which is not the case.

For *Rb. sphaeroides* a value of $\Delta H(^1P^* - {}^3P^*) = 0.411 \pm 0.003$ eV was determined from fluorescence and phosphorescence spectra[86] and, independently, from the temperature dependence of microsecond-delayed fluorescence.[87] Since one expects the entropy difference between ^{1}P* and ^{3}P* to be negligible, $\Delta G(^1P^* - {}^3P^*) \approx \Delta H(^1P^* - {}^3P^*)$, with $\Delta G_T = 0.16 \pm 0.01$ eV, a free-energy gap for charge separation to $P^+H_A^-$ of $\Delta G_{13} = \Delta G(^1P^* - P^+H_A^-) = 0.25 \pm 0.01$ eV can be calculated. From fluorescence spectra it is known that the energy of ^{1}P* in *Cf. aurantiacus* is the same as in *Rb. sphaeroides*. Due to the similarity of the primary donor,[27,29] one may also expect ^{3}P* to have similar energies in the two RCs, so that a free-energy gap for charge separation to $P^+H_A^-$, ΔG_{13}, of 0.21 ± 0.01 eV is derived for *Cf. aurantiacus* from $\Delta G_T = 0.20 \pm 0.01$ eV. These energies are depicted in Figure 5.

Energetic Inhomogeneity. Recently, RCs have been shown to be significantly inhomogeneous with respect to the free energy of $P^+H_A^-$.[47] This inhomogeneity most likely originates from differences of the interaction of the radical ions with their protein environment existing in different conformations. The energetic inhomogeneity allows one to understand the different values of ΔG_{13} obtained here and from the amplitude of delayed fluorescence. A value of $\Delta G_{13} = 0.25$ eV has been obtained

for Q_A-depleted RCs of *Rb. sphaeroides* at room temperature from the delayed fluorescence on the 10-ns time scale;[7,88,89] measurements with better time resolution and better signal-to-noise yield a slightly lower value of 0.21 eV.[47] In contrast to the results presented here, a significant decrease of ΔG_{13} to 0.08 eV upon lowering the temperature to 85 K was observed.[47] This discrepancy has been explained by the energetic inhomogeneity of $P^+H_A^-$: Predominantly those RCs with a higher energy of $P^+H_A^-$ will contribute to delayed fluorescence, which occurs after thermal repopulation of $^1P^*$ from $P^+H_A^-$. Therefore, the apparent value of ΔG_{13} determined from delayed fluorescence represents mostly those higher lying radical pairs and is smaller than the average value. Obviously, this selectivity to high-lying states is stronger at low temperatures, explaining the significant decrease of the apparent value of ΔG_{13} derived from delayed fluorescence.

Transient absorbance measurements necessarily reflect the bulk of the sample, if the energetic inhomogeneity is static on the time scale of the measurement. Such a static inhomogeneity would lead to an inhomogeneous decay of $^3P^*$ via $P^+H_A^-$. The width of the energetic distribution of $P^+H_A^-$ in RCs of *Rb. sphaeroides* has been estimated to be $2\sigma \approx 0.1$ eV.[47] Similar results were obtained for Q_A-depleted RCs of *Cf. aurantiacus*.[90] Using these values and eq 4, a distribution of τ_3 ranging from 20 to 90 μs for *Rb. sphaeroides* and from 40 to 80 μs for *Cf. aurantiacus* has to be expected at room temperature, if the energetic inhomogeneity of $P^+H_A^-$ persists up to the 100-μs time scale. Indeed, the decay of $^3P^*$ was found to be nonexponential, with distributions of τ_3 ranging from 35 to 78 μs for *Rb. sphaeroides* and from 56 to 103 μs for *Cf. aurantiacus*, as roughly estimated from biexponential fits of the $^3P^*$ decay.[91] These experimental values compare well with the distributions expected from the energetic inhomogeneity. The other mechanism contributing to the nonexponentiality of the $^3P^*$ decay, namely, the inhomogeneity of RCs with respect to the nuclear spin configuration in the case of slow NSLR, can be shown to yield only minor contributions; see the Appendix. On the other hand, significant fluctuations of protein conformations corresponding to different radical pair energies could occur on the time scale of the $^3P^*$ decay. In this case, the magnetic-field-dependent decay of $^3P^*$ would proceed predominantly via low-lying radical pair states, leading to an underestimation of the average energy of $P^+H_A^-$. In addition, the decay of $^3P^*$ would proceed monoexponentially, since it would occur with the same (time-averaged) rate constant in all RCs. This does not agree with the experimental results. We conclude that most of the inhomogeneity of protein conformations responsible for the energetic inhomogeneity of $P^+H_A^-$ on the nanosecond time scale persists up to the 100-μs time scale. Therefore, transient absorbance measurements, which yield the kinetics of radical pairs near the maximum of the distribution, directly reflect the average energetics of radical pairs in the bulk of the RC sample. On the other hand, the apparent values obtained from delayed fluorescence must not be taken literally, since they do not represent the average energetics of the radical pairs.

Energetic Relaxations. Relaxations of the cofactors or the surrounding protein resulting in a reduction of the energy of $P^+H_A^-$ at intermediate times after charge separation have been proposed to explain the observed multiphasic fluorescence decay.[92] An alternative explanation is the energetic inhomogeneity of $P^+H_A^-$, which will result in a broad distribution of the primary charge separation rate.[3,47] In contrast to energetic relaxations of $P^+H_A^-$, this effect also accounts for the dispersive kinetics of charge separation[39−43] as well as the multiphasic fluorescence decay in Q_A-containing RCs,[93] which extends to the nanosecond time scale despite the fast electron transfer from $P^+H_A^-$ to $P^+Q_A^-$ with a bulk average time constant of 200 ps.[30,66] Thus, because of the slow charge separation components arising from the energetic dispersion, it was not possible so far to unambiguously identify possible effects of energetic relaxations, although they may exist.[94]

In a recent report evidence was claimed from transient absorbance measurements on the picosecond time scale that the energy of $P^+H_A^-$ in RCs of *Rb. sphaeroides* immediately after charge separation is higher than deduced from our measurements.[95] However, for the analysis of the observed multiexponential data the authors had to include the relative amplitude of delayed fluorescence components. Thus, it is not surprising that their analysis yielded results similar to those obtained from fluorescence data. Obviously, also these results are not conclusive in the light of the energetic inhomogeneity of radical pair states.

The Energetics of $P^+B_A^-$. The recombination dynamics of $P^+H_A^-$ gives access to the lower limit of the free-energy difference $\Delta G_{23} = \Delta G(P^+B_A^- - P^+H_A^-)$. If hopping between $P^+H_A^-$ and $P^+B_A^-$ was sufficiently fast, that is, on the nanosecond time scale, various observables of the recombination dynamics would be affected.[15,96,97] In this context the additional thermally activated triplet recombination channel via $^3(P^+B_A^-)$, leading to an effective recombination rate

$$k_T = k_T^H + k_T^B \, e^{-\Delta G_{23}/k_B T} \qquad (6)$$

gives the best access to ΔG_{23}. Here, k_T^H and k_T^B denote the rate of direct recombination to $^3P^*$ from $^3(P^+H_A^-)$ and $^3(P^+B_A^-)$, respectively. The equilibrium population of $P^+B_A^-$ on the nanosecond time scale is negligible compared to $P^+H_A^-$ even at room temperature,[19,20,46] so that ΔG_{23} has to be larger than at least $2k_BT$. Thus, the second term in eq 6 decreases significantly upon decreasing the temperature. Experimentally we found an increase of k_T with decreasing temperature in RCs of *Cf. aurantiacus* and *Rb. sphaeroides*, Figure 4. This points to an inverted temperature dependence of k_T^H. However, even with k_T^H in the activationless limit, the second term in eq 6 cannot contribute more than 20% at room temperature to yield the observed inverted increase of k_T upon decreasing the temperature.

The electronic coupling between $^3(P^+B_A^-)$ and $^3P^*$ is expected to be similar to the coupling between $^1(P^+B_A^-)$ and $^1P^*$, which was estimated from the activationless rate of primary charge separation to be about 20 cm^{-1} in RCs of *Rb. sphaeroides*.[10,16] This is larger by a factor of 20 than the electronic coupling V_T between $^3(P^+H_A^-)$ and $^3P^*$; see below. Triplet recombination from $P^+H_A^-$ is near the activationless case; triplet recombination from $P^+B_A^-$, on the other hand, has a larger free-energy gap, but is not expected to have a larger reorganization energy. Thus, k_T^B is in the inverted region, but is close to the activationless case as long as $P^+B_A^-$ does not have a very large free energy. Therefore, the Franck−Condon factor for k_T^B is expected to be similar to that of k_T^H; a decrease by at most a factor of 2 will be assumed here. Since k_T^H gives the major contribution to k_T, it can be concluded that $k_T^B \geq (20)^2/2k_T^H \approx 200$ ns^{-1}.

With this lower limit of k_T^B and the upper limit of $0.2k_T$ for the second term in eq 6, a lower limit for ΔG_{23} of 0.17 eV can be estimated for *Rb. sphaeroides*. Due to the slightly slower primary charge separation, the corresponding calculation yields $\Delta G_{23} > 0.16$ eV for *Cf. aurantiacus*. The error of these values due to the uncertainty of the parameters used in the calculation

can be estimated to be less than 0.02 eV. In ref 15 a lower limit for ΔG_{23} of 0.23 eV had been deduced from the temperature dependence of the exchange interaction J in RCs of *Rb. sphaeroides*. This value, however, was based on an overestimate of the experimental accuracy in determining J[97] and may suffer from complications arising from a more thorough theoretical treatment of J.[98] Therefore, we consider the approach to ΔG_{23} given here as the most reliable one.

As a consequence, the free energy gap $\Delta G_{12} = \Delta G(^1P^* - P^+B_A^-)$ for charge separation to $P^+B_A^-$ can be estimated to be smaller than 0.05 ± 0.02 eV in *Cf. aurantiacus* and smaller than 0.08 ± 0.02 eV in *Rb. sphaeroides*. In a recent investigation[22] an effort has been made to determine ΔG_{12} in RCs of *Rb. sphaeroides*, in which the BPheo has been exchanged against a pheophytin (Pheo). Due to the larger free energy of P^+Pheo^-, a significant population of $P^+B_A^-$ is observed during the lifetime of P^+Pheo^-. From a detailed analysis of the observed transient absorbance changes, a value of ΔG_{12} of about 0.06 eV was derived. However, the free energy of P^+Pheo^- necessary for this determination was taken from the amplitude of the 300-ps-delayed fluorescence. Contributions to this fluorescence component not originating from the radical pair state (i) and an inhomogeneity of ΔG_{12} (ii) both lead to an underestimation of the true average value of ΔG_{12}, so that the value of 0.06 eV actually represents a lower limit of ΔG_{12}. Together with the upper limit derived here, the value of ΔG_{12} can be confined to $0.06 \text{ eV} < \Delta G_{12} < 0.08$ eV. These results are included in Figure 5.

VI. Discussion

In the framework of nonadiabatic electron-transfer theory, the simplest expression for the electron-transfer rate k_{ET} in the high-temperature limit (considering only vibronic modes with frequency $\hbar\omega << k_BT$) is given by the electronic coupling matrix element V, the free energy of the reaction ΔG, and the reorganization energy λ:[1]

$$k_{ET} = \frac{2\pi}{\hbar} \frac{V^2}{(4\pi\lambda k_B T)^{1/2}} e^{-E_A/k_BT} \tag{7a}$$

with the activation energy

$$E_A = \frac{(\Delta G + \lambda)^2}{4\lambda} \tag{7b}$$

If, however, high-energy modes with $\hbar\omega > k_BT$ effectively couple to the electron transfer, eq 7 needs to be altered, with major differences arising mostly in the inverted region ($-\Delta G > \lambda$).[99]

The Singlet Recombination Rate k_S: A Rate in the Marcus Inverted Region. Recombination to the singlet ground state from $^1(P^+H_A^-)$ in principle can proceed via direct recombination with the rate k_S or via thermal activation to $^1P^*$ and subsequent deactivation to P. However, due to the large free-energy gap between $P^+H_A^-$ and $^1P^*$, only a negligible fraction of 4×10^{-3} of the RCs of *Rb. sphaeroides* recombine via $^1P^*$ at room temperature.[5] In a similar way, a fraction of less than 4×10^{-2} of the RCs of *Cf. aurantiacus* can be estimated to recombine via $^1P^*$, using $k_1 = 1/(7 \text{ ps})$ for primary charge separation,[39] $\Phi_{CS} > 0.95$ for the quantum yield of charge separation,[32] and an average free energy gap $\Delta G_{13} = 0.21$ eV. Although larger than for *Rb. sphaeroides*, this contribution to singlet recombination still can be neglected.

The free energy of recombination of $P^+H_A^-$ to the ground state is about -1.1 eV ≈ -9000 cm^{-1}, Figure 5. The reorganization energy λ_S is expected to be similar to that for triplet recombination, that is, 1000−1500 cm^{-1}; see below. Thus, k_S is a rate deep in the Marcus inverted region ($-\Delta G >> \lambda$). From eq 7, a reduction of the rate by many orders of magnitude is expected upon lowering the temperature from 290 to 90 K. However, in *Cf. aurantiacus* as well as in *Rb. sphaeroides* k_S has only a weak temperature dependence, decreasing by a factor of less than 3 between 290 and 90 K. This provides clear evidence that coupling to high-energy vibronic modes in the ground state is essential, which dominates the rate especially in the inverted region, thereby diminishing its temperature dependence to a large extent.[99]

Similarity of Recombination Dynamics in *Cf. aurantiacus* and *Rb. sphaeroides*. *The Triplet Recombination Rate k_T.* Figure 4 shows the temperature dependence of the MARY width ΔB for *Cf. aurantiacus* and *Rb. sphaeroides*. On the right-hand ordinate of Figure 4, ΔB is converted directly to the triplet recombination rate k_T under the approximation of ΔB being dominated by the homogeneous width due to k_T. As discussed above, explicit numerical simulations confirmed the validity of this approximation. In both RCs, k_T has an inverted temperature dependence; that is, k_T increases upon decreasing the temperature. This shows triplet recombination to be an activationless (or close to activationless) process. Here, thermal contraction effects altering the electronic coupling V_T upon changing the temperature are neglected. In light of the small changes of the radical pair lifetime observed under high pressure (up to 345 MPa, causing a 16% decrease in sample volume),[100] such effects indeed are expected to be small.

Also shown in Figure 4 is the expected temperature dependence of k_T, calculated with eq 7 for various values of λ_T. The temperature dependence $\Delta G_T(T) = \Delta H_T - T\Delta S_T$, as determined above and linearly extrapolated to lower temperatures, was taken into account for these simulations. The electronic coupling V_T, assumed to be independent of temperature, was scaled to obtain the same value of k_T at room temperature for all simulations. The strong coupling of electron transfer to high energy vibronic modes does not significantly affect the electron transfer rate k_T, which is close to the activationless case.[99] For both RCs the measured temperature dependence of k_T is reasonably well reproduced for the same value of λ_T of about 1200 cm^{-1}. For *Cf. aurantiacus* the temperature dependence of ΔG_T drives k_T toward the activationless limit ($\Delta G_T \approx \lambda_T$) at around 100 K and introduces a small "activation" at room temperature ($\Delta G_T > \lambda_T$). This leads to the observed enhancement of the inverted temperature dependence of k_T, which is seen in the decrease of k_T by almost a factor of 3 upon increasing the temperature from 90 to 290 K. With the smaller value of ΔG_T for *Rb. sphaeroides* the strictly activationless case is expected near room temperature, whereas a slight activation is expected at 100 K. Thus, here the weak temperature dependence of ΔG_T leads to an almost temperature-independent triplet recombination rate. These general conclusions are also reflected by the Arrhenius-like plots of k_T, Figure 7, showing an activation energy of close to zero below 200 K for *Cf. aurantiacus* and above 200 K for *Rb. sphaeroides*. Summarizing, the different temperature dependence of k_T in *Cf. aurantiacus* and *Rb. sphaeroides* can be traced to the different free energy of $P^+H_A^-$ in the two RCs.

For the simulations it was assumed that the reorganization energy λ_T does not alter significantly when changing the temperature. As discussed below, this assumption probably is

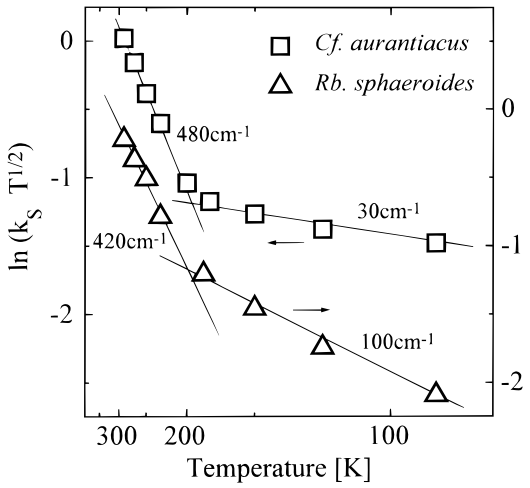

Figure 6. Arrhenius-like plot[104] of the singlet recombination rate k_S for RCs of *Cf. aurantiacus* (□, left-hand ordinate) and *Rb. sphaeroides* (△, right-hand ordinate). The size of the symbols corresponds to the error in k_S. The apparent activation energies E_A obtained from the slopes of the plots are indicated.

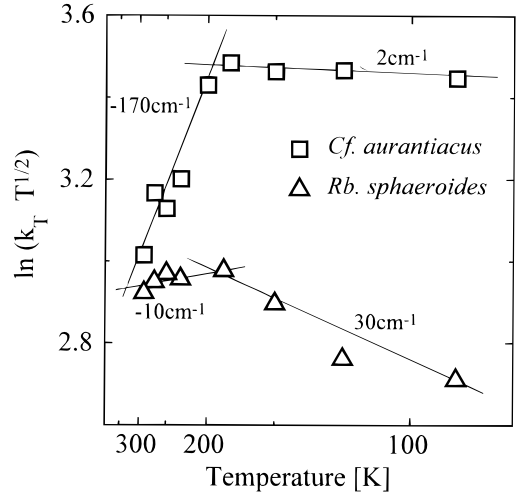

Figure 7. Arrhenius-like plot[104] of the triplet recombination rate k_T for RCs of *Cf. aurantiacus* (□) and *Rb. sphaeroides* (△). The size of the symbols corresponds to the error in k_T. The apparent activation energies E_A obtained from the slopes of the plots are indicated.

not valid around 200 K, where a conformational transition of the protein is observed. On the other hand, the discontinuity of λ_T at 200 K cannot be too large, since the value of k_T does not show a significant discontinuity (Figures 4 and 7). Taking into account the effects of a possible discontinuity of λ_T at 200 K and the uncertainty of the temperature dependent values of ΔG_T (especially below 200 K, where the values were obtained by extrapolation from high temperatures), the value of λ_T can be concluded to be in the range 1000−1500 cm^{-1} in both RCs, *Cf. aurantiacus* and *Rb. sphaeroides*.

The Recombination Matrix Elements. With the values of k_T, ΔG_T, and λ_T determined above, the electronic coupling V_T for the triplet recombination process can be calculated from eq 7. Values of $V_T = 1.0 \pm 0.2$ cm^{-1} and $V_T = 0.85 \pm 0.2$ cm^{-1} are obtained for RCs of *Cf. aurantiacus* and *Rb. sphaeroides*, respectively.

For all temperatures, k_S was found to be larger in *Cf. aurantiacus* than in *Rb. sphaeroides* by a factor of about 1.25. This larger value of k_S indicates the matrix element for singlet recombination, V_S, to be larger in *Cf. aurantiacus* than in *Rb. sphaeroides* by about 10%, since k_S is deep in the inverted region, so that the difference of the Franck−Condon factors should be insignificant.[99] This agrees well with the different values of V_T found for the two RCs.

The recombination matrix elements are dominated by superexchange coupling via $P^+B_A^-$, as predicted[10] and recently supported by experimental evidence.[47] Thus, in the simplest perturbation approach, they are given by $V = V_{PB}V_{BH}/\delta E$. Here, V_{PB} denotes the electronic coupling between $P^+B_A^-$ and P or $^3P^*$ (for V_S or V_T, respectively), V_{BH} denotes the coupling between $P^+H_A^-$ and $P^+B_A^-$, and δE is the vertical energy separation between $P^+H_A^-$ and $P^+B_A^-$ at the equilibrium nuclear coordinate of $P^+H_A^-$. The latter can be estimated from $\delta E = |\Delta G_{23}| + \lambda$, with $\Delta G_{23} = \Delta G(P^+B_A^- - P^+H_A^-)$ denoting the free-energy gap and λ the reorganization energy for $P^+B_A^- \rightarrow P^+H_A^-$. As can be seen from Figure 5, $|\Delta G_{23}|$ is 0.18 ± 0.02 eV in the case of *Rb. sphaeroides*. λ is expected to be smaller than the reorganization energy λ_T, which was determined to be in the range 1000−1500 cm^{-1}. A value of $\lambda = 800$ cm^{-1} = 0.1 eV will be assumed here.[101] Thus, δE has a value of about 0.28 eV for *Rb. sphaeroides*. In comparison, in RCs of *Cf. aurantiacus*, $P^+H_A^-$ is shifted to higher energies by 0.04 eV. Only a lower limit for the free energy of $P^+B_A^-$ could be determined for *Cf. aurantiacus*, which is 0.03 ± 0.02 eV above the free energy of $P^+B_A^-$ in *Rb. sphaeroides*; see Figure 5. If we assume the free energy of $P^+B_A^-$ to be close to this lower limit,[102] ΔG_{23} in *Cf. aurantiacus* is smaller than in *Rb. sphaeroides* by about 0.02−0.03 eV. With this smaller value of ΔG_{23} in *Cf. aurantiacus*, the recombination matrix elements are predicted to be larger by about 10% compared to *Rb. sphaeroides*, if one assumes V_{PB}, V_{BH}, and λ to be similar in the two RCs. This prediction is in good agreement with the experimental results.

In conclusion, the different recombination matrix elements in *Cf. aurantiacus* and *Rb. sphaeroides* can be explained in a self-consistent way to arise mainly from the different energetics of $P^+H_A^-$ and $P^+B_A^-$.

The Exchange Interaction J. The different energy of $P^+H_A^-$ also can be shown to be responsible for the larger value of the exchange interaction J in *Cf. aurantiacus* compared to *Rb. sphaeroides*. The exchange interaction J, the difference between the energies of $^1(P^+H_A^-)$ and $^3(P^+H_A^-)$, arises mostly from the interaction of $^1(P^+H_A^-)$ and $^3(P^+H_A^-)$ with $^1P^*$ and $^3P^*$, respectively.[2,10,12−14,16,98]

Due to its interaction with $^1P^*$, $^1(P^+H_A^-)$ is shifted to lower energies with respect to the unperturbed radical pair state. A simple perturbation treatment predicts a shift $J_S = V_S^2/\delta E_S^0$, with V_S the electronic coupling and δE_S^0 the vertical energy difference between $^1P^*$ and $P^+H_A^-$ at the equilibrium nuclear coordinate of $P^+H_A^-$ ($q = 0$, Figure 8). Because of the similar values of V_S and δE_S^0 in *Cf. aurantiacus* and *Rb. sphaeroides* the shift J_S of the singlet radical pair is expected to be very similar in the two RCs.

The corresponding shift of $^3(P^+H_A^-)$ due to its interaction with $^3P^*$ is different in the two RCs, however. In *Cf. aurantiacus* ΔG_T is larger than λ_T, so that at the equilibrium coordinate of $P^+H_A^-$ the radical pair is energetically above $^3P^*$, Figure 8. Thus, the interaction between the two states results in an upward energetic shift of $^3(P^+H_A^-)$. This is opposite to the shift of $^1(P^+H_A^-)$, and both shifts add. In contrast, for *Rb. sphaeroides* at room temperature, $\Delta G_T \approx \lambda_T$. Here, the simple perturbation treatment is not correct. An extended treatment including the effects of nuclear oscillations shows the triplet shift to be very small in this case,[98] resulting in a smaller overall

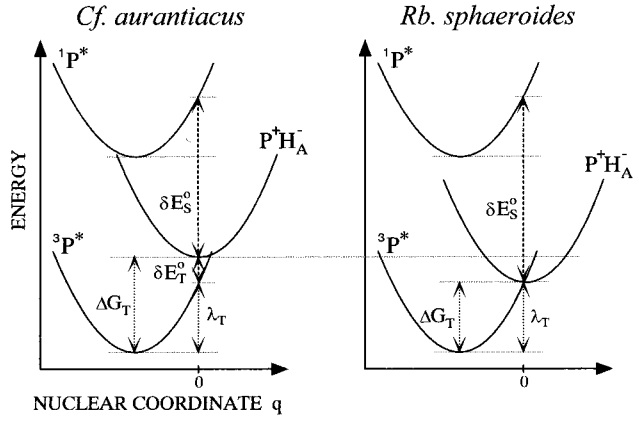

Figure 8. One-dimensional potential energy surfaces of $^1P^*$, $^3P^*$, and $P^+H_A^-$ showing the free-energy difference ΔG_T, the reorganization energy λ_T, and the vertical energy separations δE_S^0 and δE_T^0 at the equilibrium coordinate of $P^+H_A^-$ ($q = 0$) for *Cf. aurantiacus* (left) and *Rb. sphaeroides* (right) at room temperature.

energetic difference between $^1(P^+H_A^-)$ and $^3(P^+H_A^-)$ than for *Cf. aurantiacus*, in agreement with the experimental results.

From this discussion it is obvious that the sign of J is negative for *Cf. aurantiacus*; that is, $3(P^+H_A^-)$ is higher in energy than $^1(P^+H_A^-)$. No definite conclusions on the sign of J in *Rb. sphaeroides* are possible from our results, since neither the direction of the triplet shift nor the relative size of the singlet and triplet shift can be predicted accurately. Recently, the sign of J in *Rb. sphaeroides* was determined to be negative from the EPR spectrum of $P^+H_A^-$.[62]

The replacement of *Tyrosine*^{M210} by tryptophan in RCs of *Rb. sphaeroides* leads to an increase of J to twice the value found in native RCs.[63] In analogy with the above discussion, a possible mechanism for this increase is a shift of the free energy of $P^+H_A^-$ to higher values, as already suggested in ref 63. Unfortunately, no independent measurements of the altered energetics in the mutant have been performed so far.

Summary. In summary, the recombination dynamics of $P^+H_A^-$ in RCs of *Cf. aurantiacus* is very similar to that in RCs of *Rb. sphaeroides*. This is due to the close agreement in electronic coupling between the cofactors, indicating a high structural correspondence of the two RCs with respect to this radical pair and its neighborhood, and to the fairly similar energetics of the two RCs. The remaining energetic differences are the reason for the two distinct differences observed for the recombination dynamics: (i) The triplet recombination rate k_T shows a pronounced increase going to lower temperatures in *Cf. aurantiacus*, while it is almost temperature-independent in *Rb. sphaeroides*. (ii) The value of the exchange interaction J is more than twice as large in *Cf. aurantiacus* as in *Rb. sphaeroides*, which leads to the observed resonance structure of the MARY spectra, Figure 3. Also, the slightly larger recombination rates in *Cf. aurantiacus* can be traced to a larger superexchange coupling between P^+ and H_A^- due to the higher energy of $P^+H_A^-$.

This finding of close similarity of recombination dynamics extends to other RCs investigated, namely, RCs of *Rb. capsulatus* (wild-type and mutagenetically altered at position M250),[38] as well as RCs of *Rb. sphaeroides* altered at position M210.[36,38] Apparently, both structural and energetic similarity is preserved and seems to be essential for the function of the RC. Even the considerable differences that were observed between the recombination rates of bacterial RCs and photosystem II of plants could essentially be explained by the energetic differences arising from the different set of pigments, that is, chlorophyll and pheophytin instead of BChl and BPheo.[103]

Origin of the Different Energetics in *Rb. sphaeroides* and *Cf. aurantiacus*. The free energy of $P^+H_A^-$ in RCs of *Cf. aurantiacus* is larger than in RCs of *Rb. sphaeroides* by 0.04 eV. We suggest that this difference is largely due to the different amino acids at position L104, namely, polar glutamic acid in *Rb. sphaeroides* and less polar glutamine in *Cf. aurantiacus*.[24] Vibrational spectroscopy indicates hydrogen bonding of the keto oxygen at ring V of H_A with GLU^{L104} in *Rb. sphaeroides*,[33] showing this residue to be protonated. Electrostatic calculations[34,35] predict a stabilization of $P^+H_A^-$ by 0.04−0.05 eV due to the electrostatic interaction of protonated GLU^{L104} with H_A. This compares well with the observed difference between the free energy of $P^+H_A^-$ in *Rb. sphaeroides* and *Cf. aurantiacus*. However, also other amino acids might yield contributions to the different energetics. In particular, tyrosine at position M210 (TYR^{M210}) in *Rb. sphaeroides*, which is replaced by leucine in *Cf. aurantiacus*,[24] is expected (from electrostatic calculations) to yield a stabilization of $P^+H_A^-$ by about 0.02 eV.[35]

The electrostatic calculations also predict a stabilization of $P^+B_A^-$ in *Rb. sphaeroides* by TYR^{M210} by about 0.1 eV.[35] The replacement of TYR^{M210} by leucine, therefore, suggests a significantly larger free energy of $P^+B_A^-$ in *Cf. aurantiacus* compared to *Rb. sphaeroides*. However, such a conclusion ignores the effects of the replacement of other amino acid residues in the vicinity of P as well as possible structural effects due to the different sizes of tyrosine and leucine. Our results only allow us to determine lower limits for the free energy of $P^+B_A^-$, which are not too different for both RCs, but do not exclude a significantly larger value in *Cf. aurantiacus*. Interestingly, the mutagenic replacement of TYR^{M210} by phenylalanine in RCs of *Rb. sphaeroides* leads to an increase of the energy of $P^+B_A^-$ by about 0.1 eV and a smaller increase of the energy of $P^+H_A^-$.[36−38]

Conformational Transitions of the Protein. The activation energies E_A of k_S and k_T, eq 7b, can be determined from Arrhenius-like plots[104] of the rates, Figures 6 and 7. These plots show an unusual discontinuity of the temperature dependence of the recombination rates near 200 K. For temperatures above 200 K as well as below 200 K, both rates follow the temperature dependence expected from eq 7. However, at 200 K the values of the apparent activation energies change significantly. The negative apparent activation energies, which are found for k_T above 200 K, most likely are a result of the weak temperature dependence of the free energy of $P^+H_A^-$. This leads to a distortion of the temperature dependence, which is expected to be most pronounced for the close to activationless rate k_T, where $-\Delta G \approx \lambda$.

The transition temperature of 200 K corresponds to the glass point of the glycerol/buffer solution, suggesting that a slave transition of the protein, induced by the glass transition of the surrounding medium, is responsible for the observed change of activation energies at 200 K. We propose that this slave transition leads to the freezing of protein conformational fluctuations[105] and thus inhibits conformational relaxations after charge separation. One expects the new charge distribution after primary charge separation to force the protein to a new (average) conformation because of the electrostatic interaction of amino acid residues with the charged cofactors. Indeed, after cooling under illumination of Q_A-containing RCs of *Rb. sphaeroides*, altered kinetics of formation[30] and recombination[106] of $P^+Q_A^-$ have been observed. These were attributed to the different

protein conformation that the RC adopts in the state $P^+Q_A^-$ and that can be frozen in by cooling under illumination. Only after heating to temperatures above 200 K is the protein observed to return to the equilibrium conformation of the ground state.[30] This shows that below 200 K the equilibrium protein conformations for the ground and the charge-separated state do not exchange.

Consequently, after charge separation at temperatures below 200 K RCs are not expected to relax to the conformation that they adopt after charge separation to $P^+Q_A^-$ at higher temperatures. Similar conformational effects are expected after charge separation to $P^+H_A^-$, although the shorter lifetime of $P^+H_A^-$ might inhibit the complete relaxation to the equilibrium conformation for the charge-separated state. Thus, for the recombination of $P^+H_A^-$ the protein conformation is different below 200 K, where one has to expect the ground-state protein conformation, and above 200 K, where at least a partial conformational relaxation toward the charge-separated-state conformation should have occurred.

The different conformations below and above 200 K, in principle, could result in different values of the recombination matrix elements V_S and V_T, the free energy or the reorganization energy for recombination, but also in a different coupling of the recombination of $P^+H_A^-$ to high-energy modes. Conformationally induced changes of V_S and V_T would cause a discontinuity in the absolute values of both k_S and k_T at 200 K, but not alter the apparent activation energies, eq 7. No such discontinuity is observed; therefore, significantly different electronic couplings for recombination below and above 200 K seem unlikely. Significantly different values of the free energy of recombination in the two protein conformations would not be expected to significantly affect the apparent activation energy for k_S, which is a rate in the inverted region; however, they should affect the activation energy for the almost activationless k_T in a more sensitive way. Since the transition at 200 K has strong effects on the activation energies for both k_T and k_S, we exclude significantly different energetics due to protein conformational changes as the main source for the different activation energies. Thus, we tentatively suggest that the conformational relaxations mostly affect the reorganization energies λ_S and λ_T and/or the coupling to high-energy modes.

Thermally Activated Triplet Energy Transfer from ^{3}P* TO ^3B_B*. For *Rb. sphaeroides* at room temperature a good agreement between experimental and theoretical data can be found only under the assumption that the yield of recombination via the triplet channel is larger by about 40−50% than the concentration of ^{3}P* actually observed; see section IV. Similarly, in ref 107 other discrepancies were discussed which also could be resolved with the assumption that the observed concentration of ^{3}P* is smaller than the yield of recombination from $^3(P^+H_A^-)$, and an extension of the reaction scheme was proposed to account for the observed discrepancies. This assumes that $P^+H_A^-$ initially recombines much faster via the singlet channel before it relaxes in a few nanoseconds to a configuration with slower radical pair recombination. However, this scheme cannot be correct since in measurements with picosecond time resolution, no corresponding fast recovery of the Q_y absorbance of P was observed.[30,52]

We propose that the observed discrepancies arise from the fast equilibration of ^{3}P* with the triplet state of the accessory BChl B_B on the nanosecond time scale. The triplet state of B_B has been shown to be involved in the energy transfer from ^{3}P* to the carotenoid in carotenoid-containing RCs of *Rb. sphaeroides*,[108−110] which occurs on the 10-ns time scale[111] with an activation enthalpy of 0.02−0.025 eV.[112] It should be noted that B_B is located between P and the carotenoid.[8] From measurements on BChl in vitro it was concluded that the energy gap between ^{3}P* and the triplet state of the BChl monomers in the RC has a value of 0.025 eV.[86] A free-energy difference of 0.025 eV indeed corresponds to an equilibrium constant of 0.37 at room temperature, which is sufficient to account for the observed discrepancy between the concentration of ^{3}P* and the calculated yield of recombination via the triplet channel. Thus, our results indicate fast equilibration (on the nanosecond time scale or faster) between ^{3}P* and ^3B_B* in the carotenoid-free RC of *Rb. sphaeroides R26* at room temperature. This fast equilibration supports the notion that triplet energy transfer from ^{3}P* to the carotenoid actually proceeds via thermal population of ^3B_B*, which recently was deduced from measurements on RCs with modified BChls.[110]

In agreement with this proposal, no discrepancies between calculated and observed concentration of ^{3}P* are found in RCs of *Rb. sphaeroides* at low temperatures, where the equilibrium constant is significantly reduced. Furthermore, no discrepancies are found at all temperatures for RCs of *Cf. aurantiacus*, in which B_B is replaced by a BPheo.[24] The energy of the triplet state of BPheo is about 0.1 eV above that of BChl,[86] thus making it thermally inaccessible from ^{3}P*. This agreement of the concentration of ^{3}P* with the calculated yield of triplet recombination for RCs of *Cf. aurantiacus* also suggests that the triplet state of the BChl at the A-branch (B_A) cannot be populated from ^{3}P*. One may speculate, as has been done before,[113] that the geometric and energetic location of ^3B_B* in RCs of *Rb. sphaeroides* has been specifically tuned by its protein surrounding to adapt it to its function of efficiently transferring triplet energy to the close-lying carotenoid quencher to prevent the formation of harmful singlet oxygen, while such an adaptation has not taken place with ^3B_A* because of the lack of a corresponding carotenoid quencher.

Mechanism of Primary Charge Separation. The radical pair energetics and electronic couplings derived here from the magnetic-field-dependent recombination dynamics of $P^+H_A^-$ are important parameters for the discussion of the mechanism of primary charge separation. Two simple models have been discussed[2,3,10,12−23] in which electron transfer from P to H_A occurs either in two steps via B_A or directly to H_A, with B_A enhancing the electronic interaction between P and H_A via the superexchange mechanism. In principle, both mechanisms may even contribute in parallel.

In the following, we will discuss the conclusions that can be drawn on the mechanism of primary charge separation from our results. Obviously, the free energy of $P^+B_A^-$ plays a key role in deciding which mechanism dominates. Moreover, another intriguing quantity is determined from the recombination dynamics measurements, which yields information on the mechanism, namely, the exchange interaction *J*.

Exchange Interaction. Previously, the magnitude of the exchange interaction *J* has been used to draw conclusions on the mechanism of primary charge separation in RCs of *Rb. sphaeroides*.[2,10,12,13,16] From the activationless rate of primary charge separation the matrix element relevant for primary charge separation could be estimated to be about 20 cm^{-1}.[10,16] Let us first assume superexchange charge separation in one step. Then the relevant matrix element is the electronic coupling V_{PH} between ^{1}P* and $^1(P^+H_A^-)$, which is enhanced by the presence of $P^+B_A^-$. This coupling between ^{1}P* and $^1(P^+H_A^-)$ also leads to an energetic shift of $^1(P^+H_A^-)$, which is one contribution to *J*. A shift of $^1(P^+H_A^-)$ of at least 10^{-2} $cm^{-1} \approx 100$ G was

estimated.[2,10,12,13,16] This is much larger than the experimentally observed value of *J*. Two possibilities to resolve this discrepancy when assuming superexchange charge separation were discussed: (i) a fortuitous compensation of the shift of $^1(P^+H_A^-)$ by an equivalently large shift of $^3(P^+H_A^-)$ in the same direction; however, the maximum values of the triplet shift calculated with a more refined theoretical treatment[14,98] including the interaction with all vibronic states are not large enough to compensate the expected large values of the singlet shift; (ii) a fast decrease of the coupling between P and H_A due to some conformational relaxation after charge separation.[12]

On the other hand, if we assume the two-step mechanism to prevail, the electronic interaction of 20 cm^{-1} derived from the rate of primary charge separation refers to the coupling between $^1P^*$ and $P^+B_A^-$. From this, the coupling between $^1P^*$ and $^1(P^+H_A^-)$ could be estimated to be on the order of 1 cm^{-1},[10,13,16] having the same magnitude as the coupling V_T between $^3(P^+H_A^-)$ and $^3P^*$ derived above. This coupling yields a singlet shift which is well-compatible with the observed value of *J*.

In summary, while a two-step mechanism is compatible with the observed magnitude of *J* for RCs of *Rb. sphaeroides* without any restrictions, superexchange charge separation can only be reconciled with this magnitude, if conformational relaxations are assumed which lead to a dramatic decrease of the electronic coupling between P and H_A after charge separation, even at low temperatures.

The same conclusions can be drawn for *Cf. aurantiacus* at physiological temperatures. Although the rate of charge separation is slightly smaller[39,40] and the exchange interaction slightly larger than for *Rb. sphaeroides*, again their values can be reconciled with superexchange charge separation, only if conformational relaxations lead to a decrease of the electronic coupling between P and H_A after charge separation. On the other hand, for two-step charge separation the values agree well. At low temperatures charge separation in *Cf. aurantiacus* proceeds biexponentially with time constants of 2 and 25 ps.[39,41,42] For the fast component, again the assumption of superexchange charge separation leads to a discrepancy between fast charge separation rate and small exchange interaction, if no conformational relaxations are present. In principle, the slow component, arising from RCs with energetically high lying $P^+B_A^-$, may be compatible with the superexchange mechanism without making assumptions on conformational relaxations.

Free Energy of $P^+B_A^-$. More detailed conclusions can be drawn from the energetics of $P^+B_A^-$. Recently, all observed rates have been modeled for native and modified RCs of *Rb. sphaeroides* within the framework of nonadiabatic electron-transfer theory.[2,3,114] The two-step mechanism was found to dominate as long as the free energy of $P^+B_A^-$ is below that of $^1P^*$.

The discussion of primary charge separation is complicated by the energetic inhomogeneity of radical pair states.[3,47] For *Rb. sphaeroides*, it was shown that the free energy of $P^+H_A^-$ has a distribution with a width σ (hwhm) of about 0.05 eV. A similar energetic inhomogeneity is to be expected for $P^+B_A^-$. It was proposed that these energetic inhomogeneities lead to the observed deviations of charge separation from monoexponentiality.[3,47,115]

Transient absorbance measurements, as employed here, yield the bulk average values of the free energies. For *Rb. sphaeroides*, the free energy of $P^+B_A^-$ was found to be 0.06−0.08 eV below $^1P^*$, Figure 5. Even for a distribution with a width of 0.05 eV (hwhm), the free energy of $P^+B_A^-$ is significantly below that of $^1P^*$ for most of the RCs, resulting in two-step charge separation at all temperatures.[2,3,114] This conclusion is in agreement with recent experimental results.[19−23] To obtain more quantitative results, we simulated the distribution of the rate of primary charge separation, using eq 7 and a Gaussian distribution of ΔG_{12} around 0.07 eV with a width of 0.05 eV. Since the observed primary charge separation rate is activationless, the reorganization energy λ_1 was assumed to be close to the average value of ΔG_{12}. These simulations show that for the majority of RCs of *Rb. sphaeroides* indeed no significant activation of two-step charge separation is expected. Furthermore, these simulations yield only small deviations from exponentiality in the bulk charge separation process.

The free energy of $P^+B_A^-$ in *Cf. aurantiacus* is at most 0.05 eV below that of $^1P^*$ and thus is closer to the free energy of $^1P^*$ than in *Rb. sphaeroides*. This makes primary charge separation more sensitive to the energetic inhomogeneity. The width of the energetic distribution of radical pairs in *Cf. aurantiacus* is similar to that in *Rb. sphaeroides*.[90] Thus, in *Cf. aurantiacus* the free energy of $P^+B_A^-$ in a significant portion of RCs is expected to be close to or even above that of $^1P^*$. This leads to a high activation barrier in the two-step model, which can explain the observed more pronounced nonexponential kinetics in RCs of *Cf. aurantiacus*,[39−42] increasing toward lower temperatures. Calculations with eq 7, using the same reorganization energy, electronic coupling, and width of distribution of ΔG_{12} as for *Rb. sphaeroides*, but an average free energy of $P^+B_A^-$ higher by only 0.02 eV, indeed yield distributions of the charge separation rate at 100 and 300 K that are similar to the experimental observations. Since these calculations are based on the two-step model, they indicate that also in *Cf. aurantiacus* charge separation proceeds in two steps in the majority of RCs, even at low temperatures. Only for RCs at the extreme high-energy wing of the energetic distribution would the two-step process be slowed down to such an extent that charge separation would be governed by the superexchange mechanism. This effect increases toward low temperatures.

VII. Conclusions

The radical pair energetics relevant for primary charge separation were determined from highly precise transient absorbance measurements of the spin-dependent recombination dynamics of $P^+H_A^-$ and the lifetime of the recombination product $^3P^*$. Because of the energetic inhomogeneity of radical pairs, no other method allows an unambiguous determination of the energetics, which is a necessary prerequisite for the discussion of primary charge separation.

Measurements were performed on the RC of *Rb. sphaeroides* and, for the first time with comparable completeness and accuracy, on another RC, that of *Cf. aurantiacus*, to test the universality of the energetics and mechanism of primary charge separation. The recombination dynamics of $P^+H_A^-$ in *Cf. aurantiacus* and *Rb. sphaeroides* were found to be similar. The differences, which are the larger exchange interaction and the stronger temperature dependence of the rate k_T in *Cf. aurantiacus*, can be explained by the observed different free energy of $P^+H_A^-$ alone. We attribute this different energy largely to the different amino acid at position L104, namely, glutamic acid in *Rb. sphaeroides* and glutamine in *Cf. aurantiacus*.

In both RCs, the energetic inhomogeneity of $P^+B_A^-$ could lead to the parallel occurence of activationless and activated two-step charge separation. The free energy gap for primary charge separation to $P^+B_A^-$ is found to be smaller in *Cf. aurantiacus*. From this we predict more significant deviations

of charge separation from monoexponentiality, which indeed is in agreement with the experimental results.

Acknowledgment. We are very grateful to Prof. M. Bixon and Prof. J. Jortner for continuous collaboration and stimulating discussions. Financial support from the Deutsche Forschungsgemeinschaft (Sonderforschungsbereich 143) is gratefully acknowledged.

Appendix: Influence of Nuclear Spin Polarization on the Decay of ^{3}P*

In the following, we will discuss the effects of a nonrandom distribution of the nuclear spin configurations on the decay of ^{3}P*. For all simulations described here, the energy of $P^+H_A^-$ was assumed to have one definite value in all RCs. This allows us to separate the effects of the nuclear spin configurations from the effects of the energetic inhomogeneity of $P^+H_A^-$.

In thermodynamic equilibrium the nuclear spins are oriented statistically, leading to a distribution $f^0(\omega,B)$ of the S−T mixing frequency, ω, of the radical pair $P^+H_A^-$. $f^0(\omega,B)$ depends on the presence of an external magnetic field, B, since for large values of B only the z-component of the hyperfine field contributes to the mixing.[116] Because of reversibility, the T−S mixing frequency for a certain nuclear spin configuration is identical to the S−T mixing frequency. Formation of ^{3}P* via the radical pair mechanism initially leads to a nonequilibrium distribution of the nuclear spin configurations in ^{3}P* (nuclear spin polarization, NSP), since ^{3}P* is preferentially formed in RCs with strong S−T mixing. The distribution $f^3(\omega,B)$ of ω corresponding to this initial distribution of the nuclear spin configurations is given by[116]

$$f^3(\omega,B) = Nf^0(\omega,B)\,\Phi_T(\omega,B) \tag{A1}$$

Here $\Phi_T(\omega,B)$ denotes the yield of ^{3}P* for RCs with a S−T mixing frequency ω and N is a normalization factor ensuring the integral of $f^3(\omega,B)$ over ω to be unity.

Fast Nuclear Spin Relaxation. The triplet radical pair $^3(P^+H_A^-)$ is in thermal equilibrium with ^{3}P* and is repopulated many times before T−S mixing and recombination to the ground state occur, as can be seen from the values of k_{-T} ($\approx 1\ \mu s^{-1}$)[5] and τ_3. If nuclear spin lattice relaxation (NSLR) is considerably faster than the decay of ^{3}P*, the nuclear spin configuration of each RC in ^{3}P* will change rapidly so that the T−S mixing frequency ω for different repopulation events will be different, with the probability of a certain frequency given by the equilibrium distribution $f^0(\omega,B)$. The average depopulation rate of ^{3}P* then can be calculated from

$$\langle k_3(B)\rangle_\omega = \int k_3(\omega,B)\, f^0(\omega,B)\, d\omega = k_{ISC} + \frac{1}{3} k_S \langle \Phi_T(\omega,B)\rangle_\omega e^{-\Delta G_T/k_B T} \tag{A2}$$

with $k_3(\omega,B)$ the depopulation rate for a certain nuclear spin configuration, given by eq 4, and $\langle ...\rangle_\omega$ indicating the average over the equilibrium distribution of ω. As can be seen, the use of eqs 4 and 5 for the determination of ΔG_T is justified in this case, since the experimentally determined value of $\Phi_T(B)$ corresponds to the average value $\langle \Phi_T(\omega,B)\rangle_\omega$. Since all RCs will decay with the *same* average rate $\langle k_3(B)\rangle_\omega$, the decay of ^{3}P* should be monoexponential. However, as discussed in detail in the text, the energetic inhomogeneity of $P^+H_A^-$ still will cause deviations from monoexponentiality.

Slow Nuclear Spin Relaxation. In fact, the deviation of the value of τ_3 at zero magnetic field from the linear dependence of $\tau_3(\Phi_T)$ observed at high magnetic fields[6] indicates that NSLR is not significantly faster than the decay of ^{3}P*. For slow NSLR, the RCs in the state ^{3}P* are inhomogeneously distributed with respect to their nuclear spin configuration, and the decay of ^{3}P* via $P^+H_A^-$ would be nonexponential even without the energetic inhomogeneity of $P^+H_A^-$. The average lifetime of ^{3}P* can be calculated from

$$\langle \tau_3(B)\rangle_\omega = \int \frac{1}{k_3(\omega,B)} f^3(\omega,B)\, d\omega = \int \frac{1}{k_{ISC} + (1/3)k_S \Phi_T(\omega,B) e^{-\Delta G_T/k_B T}} f^3(\omega,B)\, d\omega \tag{A3}$$

In principle, a fit of the observed values of τ_3 at 0 and 700 G to eq A3 allows one to take into account the effects of NSP in the evaluation of ΔG_T. However, the dependence of Φ_T on ω is not experimentally accessible, and one has to refer to theoretical models. From the Hamiltonian and the stochastic Liouville equation,[73] $\Phi_T(\omega)$ only can be obtained with extensive numerical calculations, so that a fit of the data using this model is not feasible. In ref 5, the one-proton model[55] was used for the calculation of $\Phi_T(\omega)$ and the evaluation of ΔG_T. However, due to its simplifications this model does not reproduce the experimentally observed triplet yields very well. Thus, it actually is not suited to obtain exact results for ΔG_T from the experimental data.

In the following we will use this model for simpler numerical simulations which show that the effect of NSP on τ_3 is small. Furthermore, these simulations show that the error introduced by the neglect of NSP in the determination of ΔG_T is small.

Numerical Simulations. In the semiclassical model of radical pair recombination,[75] each radical spin precesses around a classical magnetic field, which is the sum of the applied external field $\mathbf{B}$ and the hyperfine fields $\mathbf{B_1}$ and $\mathbf{B_2}$ at P^+ and H_A^-, respectively. The large number of possible nuclear spin configurations can be described by a Gaussian distribution of the field at each radical with a width that can be determined from the HFI-induced EPR widths of P^+ and H_A^-. The distribution of the HFI fields leads to a corresponding distribution of the S−T mixing frequency ω.

$$\omega = \frac{g\beta}{\hbar}|\mathbf{B_1} - \mathbf{B_2}| \tag{A4}$$

From the distribution[75] of $\mathbf{B_1}$ and $\mathbf{B_2}$ one obtains the equilibrium distribution $f^0(\omega,B)$:[117]

$$f^0(\omega,B) = \frac{8\omega^2}{(2\pi)^{1/2}\omega_{eff}^3} e^{-2\omega^2/\omega_{eff}^2} \qquad B = 0$$

$$= \frac{1}{(\pi/2)^{1/2}\omega_{eff}} e^{-2\omega^2/\omega_{eff}^2} \qquad B = B_{sat} \tag{A5}$$

with $\omega_{eff} = (g\beta/\hbar)A_{eff}$ and $A_{eff} = (A_P^2 + A_H^2)^{1/2} = 16$ G, as calculated from the HFI-induced EPR widths[76,77] $A_P = 9.5$ G of P^+ and $A_H = 13$ G of H_A^-. Here, B_{sat} denotes a magnetic field at which HFI-induced S−T mixing is completely saturated, but Δg-induced S−T mixing is not yet significant; that is, B_{sat} is on the order of several 100 G.

In the following, we will use the one-proton model, in which HFI is described by the interaction of one of the radical electron

TABLE 3: Results of Numerical Simulations of the Effect of NSP on the Lifetime of $^3P^*$[a]

input parameters				calculated triplet yields, eq A6		fast NSLR, eq A2			slow NSLR, eq A3		
k_{ISC} [10^4 s^{-1}]	k_S [10^7 s^{-1}]	k_T [10^9 s^{-1}]	ΔG_T [eV]	$\langle\Phi_T^0\rangle_A$	$\langle\Phi_T^{sat}\rangle_A$	τ_3^0 [μs]	τ_3^{sat} [μs]	ΔG_T^{fast} [eV]	τ_3^0 [μs]	τ_3^{sat} [μs]	ΔG_T^{slow} [eV]
1	6	1	0.200	0.254	0.125	85.42	92.26	0.200	81.99	85.44	0.214
			0.180			72.47	84.27	0.180	67.80	73.35	0.194
			0.220			92.88	96.37	0.220	90.87	92.73	0.234
0.5	6	1	0.200	0.254	0.125	149.1	171.3	0.200	140.0	150.5	0.214
1	9	1	0.200	0.191	0.091	83.89	91.58	0.200	79.6	83.58	0.213
1	6	1.5	0.200	0.232	0.114	86.51	92.92	0.200	83.19	86.27	0.215

[a] Input parameters: k_{ISC} rate of intersystem crossing for $^3P^*$; k_S and k_T singlet and triplet recombination rate of $P^+H_A^-$; ΔG_T free-energy gap between $P^+H_A^-$ and $^3P^*$. The exchange interaction J was fixed to 25 G for all simulations. Simulation results: $\langle\Phi_T^0\rangle_A$ and $\langle\Phi_T^{sat}\rangle_A$ average triplet yield for $B = 0$ and $B = B_{sat}$, respectively, eq A6; τ_3^0 and τ_3^{sat} simulated lifetime of $^3P^*$ for $B = 0$ and $B = B_{sat}$, respectively, eq A2 (fast NSLR) or eq A3 (slow NSLR); ΔG_T^{fast} and ΔG_T^{slow} free-energy gap between $P^+H_A^-$ and $^3P^*$, calculated with eq 5 from the simulated values of τ_3 and $\langle\Phi_T\rangle_A$.

spins with a nuclear spin 1/2 with HFI constant A. In this model, the triplet yield $\Phi_T(A,B)$ is given by[55]

$$\Phi_T(A,B) = \frac{3A^2k_T(k_T + k_S)}{(3A^2 + 4k_Sk_T)(k_S + k_T)^2 + 16k_Sk_T(J - A/2)^2} \qquad B = 0$$

$$= \frac{A^2k_T(k_T + k_S)}{(A^2 + 4k_Sk_T)(k_S + k_T)^2 + 16k_Sk_TJ^2} \qquad B = B_{sat} \quad \text{(A6)}$$

We will model the distribution of nuclear spin configurations by assuming a distribution of the HFI constant A. The distribution of A is chosen to yield the same distribution of mixing frequencies ω as the semiclassical model, eq A5. In the one-proton model, the mixing frequency is $\omega = (g\beta/\hbar)A$ for $B = 0$ and $\omega = (g\beta/\hbar)A/2$ for $B = B_{sat}$.[118] Therefore, we assume the following equilibrium distribution of A:

$$f^0(A,B) = \frac{8A^2}{(2\pi)^{1/2}A_{eff}^3}\, e^{-2A^2/A_{eff}^2} \qquad B = 0$$

$$= \frac{1}{(2\pi)^{1/2}A_{eff}}\, e^{-A^2/2A_{eff}^2} \qquad B = B_{sat} \quad \text{(A7)}$$

Using these distributions of A together with eq A6 results in average triplet yields $\langle\Phi_T\rangle_A$ which compare reasonably well with the experimental results and with results of more thorough numerical simulations, both for $B = 0$ and $B = B_{sat}$; see Table 3. The lifetime τ_3 of $^3P^*$ can be simulated in this model for fast and for slow NSLR from eqs A2 and A3, respectively, replacing ω by A and using eqs A1 and A6. Results obtained for values of the parameters k_{ISC}, k_S, k_T, and ΔG_T typical for *Cf. aurantiacus* are collected in Table 3. As expected, NSP (persisting in the case of slow NSLR) accelerates the decay of $^3P^*$; the value of τ_3 calculated for slow NSLR is found to smaller by 5−15% than the value calculated for fast NSLR.

We determined ΔG_T from our experimental results using eq 5, which is identical to eq A2, that is, assumes fast NSLR, despite the slow NSLR which is indicated by the comparison of high- and low-field experiments. The above simulations allow one to directly obtain an estimate of the error introduced by neglecting slow NSLR. Values for ΔG_T calculated from the simulated values of τ_3 and $\langle\Phi_T\rangle$ with eq 5 are included in Table 3. Of course, the data simulated under the assumption of fast NSLR exactly reproduce the input value of ΔG_T. The data simulated under the assumption of slow NSLR, on the other hand, yield slightly higher values for ΔG_T. However, in all cases, the error is smaller than 0.015 eV. Calculations using input parameters typical for *Rb. sphaeroides* allow the same conclusion (data not shown).

Comparison with High-Field Measurements. In principle, the distorting effect of NSP can be avoided by measurements in high magnetic fields, where S−T mixing is mostly due to the Δg effect. Indeed, such measurements[6] yielded a linear dependence of τ_3 on Φ_T in RCs of *Rb. sphaeroides*, as expected from eq 4 in the absence of NSP effects. The observed value of τ_3 at 0 G deviates from this linear dependence, indicating effects from NSP and, therefore, slow NSLR. However, the observed deviation is small. The decay of $^3P^*$ at 0 G was found to be 7% faster than expected from the extrapolation of the high-field data.

From our simulations one would expect an *over*estimation of ΔG_T from low-field data evaluated neglecting NSP. However, the value of ΔG_T in RCs of *Rb. sphaeroides* at room temperature determined from high-field data[6] (0.170 eV) is *larger* than the value determined from our low-field data (0.155 eV). Part of this discrepancy actually is due to the different values for k_S used in ref 6 and here. After correcting for this difference, the values agree within experimental uncertainties. Thus, we conclude that the effect of NSP on the decay of $^3P^*$ actually is smaller than suggested by our simulations, which were performed under the assumption of no NSLR. This conclusion is further supported by the observation of a photochemically induced dynamic nuclear polarization signal in NMR spectra of RCs of *Rb. sphaeroides*,[85] which indicates some NSLR to occur within the lifetime of $^3P^*$. Thus, the use of eq 5 for the determination of ΔG_T is well-justified.

Deviations from Monoexponentiality for Slow NSLR. Using the model described above, it is possible to calculate numerically the distribution $f(\tau_3)$ of the $^3P^*$ lifetime $\tau_3(\omega,B) = 1/k_3(\omega,B)$ (compare eq A3) for the case of slow NSLR from the distribution $f^3(\omega,B)$ of the S−T mixing frequency, ω. The corresponding simulated time dependence of $^3P^*$ decay (obtained from $f(\tau_3)$ by numerical Laplace transformation) shows only minor deviations from monoexponentiality. When using parameters typical for *Rb. sphaeroides*, a biexponential fit of the simulated $^3P^*$ decay yields time constants of typically 45 and 60 μs. Thus, the contribution of the inhomogeneous distribution of nuclear spin conformations to the nonexponentiality of $^3P^*$ decay is significantly smaller than the experimentally observed nonexponentiality. It can be concluded that the latter is governed by the energetic inhomogeneity of $P^+H_A^-$.

References and Notes

(1) (a) Jortner, J. *Biochim. Biophys. Acta* **1980**, *594*, 193. (b) Marcus, R.A.; Sutin, N. *Biochim. Biophys. Acta* **1985**, *811*, 265.

(2) Bixon, M.; Jortner, J.; Michel-Beyerle, M. E. *Biochim. Biophys. Acta* **1991**, *1056*, 301.
(3) Bixon, M.; Jortner, J.; Michel-Beyerle, M. E. *Chem. Phys.* **1995**, *197*, 389.
(4) Chidsey, C. E. D.; Takiff, L.; Goldstein, R. A.; Boxer, S. G. *Proc. Natl. Acad. Sci. U.S.A.* **1985**, *82*, 6850.
(5) Ogrodnik, A.; Volk, M.; Letterer, R.; Feick, R.; Michel-Beyerle, M. E. *Biochim. Biophys. Acta* **1988**, *936*, 361.
(6) Goldstein, R. A.; Takiff, L.; Boxer, S. G. *Biochim. Biophys. Acta* **1988**, *934*, 253.
(7) Ogrodnik, A. *Biochim. Biophys. Acta* **1990**, *1020*, 65.
(8) (a) Deisenhofer, J.; Epp, O.; Miki, K.; Huber, R; Michel, H. *J. Mol. Biol.* **1984**, *180*, 385. (b) Chang, C.-H.; Tiede, D.; Tang, J.; Smith, U.; Norris, J.R.; Schiffer, M. *FEBS Lett.* **1986**, *205*, 82. (c) Allen, J. P.; Feher, G.; Yeates, T. O.; Komiya, H.; Rees, D. C. *Proc. Natl. Acad. Sci. U.S.A.* **1987**, *84*, 5730.
(9) Ogrodnik, A.; Remy-Richter, N.; Michel-Beyerle, M. E. *Chem. Phys. Lett.* **1987**, *135*, 576.
(10) Bixon, M.; Jortner, J.; Michel-Beyerle, M. E.; Ogrodnik, A. *Biochim. Biophys. Acta* **1989**, *977*, 273.
(11) Volk, M. Ph.D. Thesis, Technische Universität München, 1991.
(12) (a) Marcus, R.A. *Chem. Phys. Lett.* **1987**, *133*, 471. (b) Marcus, R.A. *Chem. Phys. Lett.* **1988**, *146*, 13.
(13) Michel-Beyerle, M. E.; Bixon, M.; Jortner, J. *Chem. Phys. Lett.* **1988**, *151*, 188.
(14) Bixon, M.; Jortner, J.; Michel-Beyerle, M. E. *Z. Phys. Chem.* **1993**, *180*, 193.
(15) Bixon, M.; Jortner, J.; Michel-Beyerle, M. E.; Ogrodnik, A.; Lersch, W. *Chem. Phys. Lett.* **1987**, *140*, 626.
(16) Bixon, M.; Michel-Beyerle, M. E.; Jortner, J. *Isr. J. Chem.* **1988**, *28*, 155.
(17) Martin J. L.; Breton, J.; Hoff, A. J.; Migus, A.; Antonetti, A. *Proc. Natl. Acad. Sci. U.S.A.* **1986**, *83*, 957.
(18) (a) Kirmaier, C.; Holten, D. *Proc. Natl. Acad. Sci. U.S.A.* **1990**, *87*, 3552. (b) Chan, C. K.; DiMagno, T. J.; Chen, L. X. Q.; Norris, J.R.; Fleming, G. R. *Proc. Natl. Acad. Sci. U.S.A.* **1991**, *88*, 11202.
(19) Holzapfel, W.; Finkele, U.; Kaiser, W.; Oesterhelt, D.; Scheer, H.; Stilz, H. U.; Zinth, W. *Chem. Phys. Lett.* **1989**, *160*, 1.
(20) Lauterwasser, C.; Finkele, U.; Scheer, H.; Zinth, W. *Chem. Phys. Lett.* **1991**, *183*, 471.
(21) Arlt, T.; Schmidt, S.; Kaiser, W.; Lauterwasser, C.; Meyer, M.; Scheer, H.; Zinth, W. *Proc. Natl. Acad. Sci. U.S.A.* **1993**, *90*, 11757.
(22) Schmidt, S.; Arlt, T.; Hamm, P.; Huber, H.; Nägele, T.; Wachtveitl, J.; Meyer, M.; Scheer, H.; Zinth, W. *Chem. Phys. Lett.* **1994**, *223*, 116.
(23) (a) Häberle, T.; Lossau, H.; Friese, M.; Hartwich, G.; Ogrodnik, A.; Scheer, H.; Michel-Beyerle, M. E. In *The Reaction Center of Photosynthetic Bacteria: Structure and Dynamics*; Michel-Beyerle, M. E., Ed.; Springer-Verlag: Berlin, 1996; p 239. (b) Hartwich, G.; Bieser, G.; Langenbacher, T.; Müller, P.; Richter, M.; Ogrodnik, A.; Scheer, H.; Michel-Beyerle, M. E. *Biophys. J.* **1997**, *71*, A8.
(24) (a) Ovchinnikov, Y .A.; Abdulaev, N. G.; Zolotarev, A. S.; Shmukler, B.E.; Zargarov, A. A.; Kutuzov, M. A.; Telezhinskaya, I. N; Levina, N. B. *FEBS Lett.* **1988**, *231*, 237. (b) Ovchinnikov, Y. A.; Abdulaev, N. G.; Shmukler, B. E.; Zargarov, A. A.; Kutuzov, M. A.; Telezhinskaya, I.N.; Levina, N. B.; Zolotarev, A. S. *FEBS Lett.* **1988**, *232*, 364. (c) Shiozawa, J. A.; Lottspeich, F.; Oesterhelt, D.; Feick, R. *Eur. J. Biochem.* **1989**, *180*, 75.
(25) Blankenship, R. E.; Feick, R.; Bruce, B. D.; Kirmaier, C.; Holten, D.; Fuller, R.C. *J. Cell. Biochem.* **1983**, *22*, 251.
(26) Pierson, B. K.; Thornber, J. P. *Proc. Natl. Acad. Sci. U.S.A.* **1983**, *80*, 80.
(27) Vasmel, H.; Amesz, J.; Hoff, A. J. *Biochim. Biophys. Acta* **1986**, *852*, 159.
(28) Eberl, U. Ph.D. Thesis, Technische Universität München, 1992.
(29) Bruce, B.D.; Fuller, R.C.; Blankenship, R.E. *Proc. Natl. Acad. Sci. U.S.A.* **1982**, *79*, 6532.
(30) Aumeier, W. Ph.D. Thesis, Technische Universität München, 1990.
(31) Aumeier, W.; Eberl, U.; Ogrodnik, A.; Volk, M.; Scheidel, G.; Feick, R.; Plato, M.; Michel-Beyerle, M. E. In *Current Research in Photosynthesis*; Baltscheffsky, M., Ed.; Kluwer Academic Publishers: Netherlands, 1990; Vol. I, p 133.
(32) Volk, M.; Scheidel, G.; Ogrodnik, A.; Feick, R.; Michel-Beyerle, M. E. *Biochim. Biophys. Acta* **1991**, *1058*, 217.
(33) Lutz, M.; Robert, B. In *Antennas and Reaction Centers of Photosynthetic Bacteria: Structure, Interaction and Dynamics*; Michel-Beyerle, M. E., Ed.; Springer-Verlag: Berlin, 1985; p 138.
(34) Michel-Beyerle, M. E.; Plato, M.; Deisenhofer, J.; Michel, H.; Bixon, M.; Jortner, J. *Biochim. Biophys. Acta* **1988**, *932*, 52.
(35) Parson, W. W.; Chu, Z. T.; Warshel, A. *Biochim. Biophys. Acta* **1990**, *1017*, 251.
(36) Volk, M.; Neumann, W.; Ogrodnik, A.; Gray, K. A.; Oesterhelt, D.; Michel-Beyerle, M. E. *Biophys. J.* **1993**, *64*, A18.
(37) Nagarajan, V.; Parson, W. W.; Davis, D.; Schenck, C. C. *Biochemistry* **1993**, *32*, 12324.
(38) Volk, M.; Ogrodnik, A.; Michel-Beyerle, M. E. In *Anoxygenic Photosynthetic Bacteria*; Blankenship, R.E., Madigan, M. T., Bauer, C. E., Eds.; Kluwer Academic Publishers: Netherlands, 1995; Chapter 27, p 595.
(39) Becker, M.; Nagarajan, V.; Middendorf, D.; Parson, W. W.; Martin, J. E.; Blankenship, R. E. *Biochim. Biophys. Acta* **1991**, *1057*, 299.
(40) Hamm, P.; Gray, K. A.; Oesterhelt, D.; Feick, R.; Scheer, H.; Zinth, W. *Biochim. Biophys. Acta* **1993**, *1142*, 99.
(41) Martin, J. L.; Lambry, J. C.; Ashokkumar, M.; Michel-Beyerle, M. E.; Feick, R.; Breton, J. In *Ultrafast Phenomena VII*; Harris, C. B., Ippen, E. P., Mourou, G. A., Zewail, A. H., Eds.; Springer-Verlag: Berlin, 1990; p 524.
(42) Feick, R.; Martin, J. L.; Breton, J.; Volk, M.; Scheidel, G.; Langenbacher, T.; Urbano, C.; Ogrodnik, A.; Michel-Beyerle, M. E. In *Reaction Centers of Photosynthetic Bacteria*; Michel-Beyerle, M. E., Ed.; Springer-Verlag: Berlin, 1990; p 181.
(43) (a) Vos, M. H.; Lambry, J.-C.; Robles, S. J.; Youvan, D. C.; Breton, J.; Martin, J.-L. *Proc. Natl. Acad. Sci. U.S.A.* **1991**, *88*, 8885. (b) Vos, M. H.; Lambry, J.-C.; Robles, S. J.; Youvan, D. C.; Breton, J.; Martin, J.-L. *Proc. Natl. Acad. Sci. U.S.A.* **1992**, *89*, 613. (c) Du, M.; Rosenthal, S. J.; Xie, X.; DiMagno, T. J.; Schmidt, M.; Hanson, D. K.; Schiffer, M.; Norris, J. R.; Fleming, G. R. *Proc. Natl. Acad. Sci. U.S.A.* **1992**, *89*, 8517.
(44) Woodbury, N. W.; Becker, M.; Middendorf, D.; Parson, W. W. *Biochemistry* **1985**, *24*, 7516.
(45) Fleming, G. R.; Martin, J. L.; Breton, J. *Nature* **1988**, *333*, 190.
(46) Breton, J.; Martin, J. L.; Fleming, G. R.; Lambry, J. C. *Biochemistry* **1988**, *27*, 8276.
(47) Ogrodnik, A.; Keupp, W.; Volk, M.; Aumeier, G.; Michel-Beyerle, M. E. *J. Phys. Chem.* **1994**, *98*, 3432.
(48) Hoff, A. J. *Q. Rev. Biophys.* **1981**, *14*, 599.
(49) Boxer, S. G.; Chidsey, C. E. D.; Roelofs, M. G. *Annu. Rev. Phys. Chem.* **1983**, *34*, 389.
(50) Schenck, C. C.; Blankenship, R. E.; Parson, W. W. *Biochim. Biophys. Acta* **1982**, *680*, 44.
(51) Ogrodnik, A.; Krüger, H. W.; Orthuber, H.; Haberkorn, R.; Michel-Beyerle, M. E. *Biophys. J.* **1982**, *39*, 91.
(52) Chidsey, C. E. D.; Kirmaier, C.; Holten, D.; Boxer, S.G. *Biochim. Biopys. Acta* **1984**, *766*, 424.
(53) Norris, J. R.; Budil, D. E.; Tiede, D. M.; Tang, J.; Kolaczkowski, S. V.; Chang, C. H.; Schiffer, M. In *Progress in Photosynthesis Research*; Biggens, J., Ed.; Martinus Nijhoff Publishers: Dordrecht, 1987; Vol. I, p 363.
(54) Haberkorn, R.; Michel-Beyerle, M. E. *FEBS Lett.* **1977**, *75*, 5.
(55) Haberkorn, R.; Michel-Beyerle, M. E. *Biophys. J.* **1979**, *26*, 489.
(56) Werner, H. J.; Schulten, K.; Weller, A. *Biochim. Biophys. Acta* **1978**, *502*, 255.
(57) (a) Wasielewski, M. R.; Bock, C. H.; Bowman, M. K.; Norris, J. R. *J. Am. Chem. Soc.* **1983**, *105*, 2903. (b) Wasielewski, M. R.; Bock, C. H.; Bowman, M. K.; Norris, J. R. *Nature* **1983**, *303*, 520. (c) Wasielewski, M. R.; Norris, J. R.; Bowman, M. K. *Faraday Discuss. Chem. Soc.* **1984**, *78*, 279.
(58) Moehl, K. W.; Lous, E. J.; Hoff, A. J. *Chem. Phys. Lett.* **1985**, *121*, 22.
(59) Goldstein, R. A.; Boxer, S. G. *Biochim. Biophys. Acta* **1989**, *977*, 70.
(60) (a) Norris, J. R.; Bowman, M. K.; Budil, D. E.; Tang, J.; Wraight, C. A.; Closs, G. L. *Proc. Natl. Acad. Sci. U.S.A.* **1982**, *79*, 5532. (b) Lersch, W.; Michel-Beyerle, M. E. In *Advanced EPR. Applications in Biology and Biochemistry*; Hoff, A. J., Ed.; Elsevier: Amsterdam, 1989; p 685. (c) Lersch, W.; Lang, E.; Feick, R.; Coleman, W. J.; Youvan, D. C.; Michel-Beyerle, M. E. In *Perspectives in Photosynthesis*; Jortner, J., Pullman, B., Eds.; Kluwer Academic Publishers: Netherlands, 1990; p 81.
(61) Hore, P. J.; Riley, D. J.; Semlyen, J. J.; Zwanenburg, G.; Hoff, A. J. *Biochim. Biophys. Acta* **1993**, *1141*, 221.
(62) Proskuryakov, I. I.; Klenina, I. B.; Hore, P. J.; Bosch, M. K.; Gast, P.; Hoff, A. J. *Chem. Phys. Lett.* **1996**, *257*, 333.
(63) Van der Vos, R.; Franken, E. M.; Sexton, S. J.; Shochat, S.; Gast, P.; Hore, P. J.; Hoff, A. J. *Biochim. Biophys. Acta* **1995**, *1230*, 51.
(64) Shiozawa, J.A.; Lottspeich, F.; Feick, R. *Eur. J. Biochem.* **1987**, *167*, 595.
(65) Volk, M.; Aumeier, G.; Häberle, T.; Ogrodnik, A.; Feick, R.; Michel-Beyerle, M. E. *Biochim. Biophys. Acta* **1992**, *1102*, 253.
(66) (a) Kirmaier, C.; Holten, D.; Parson, W. W. *Biochim. Biophys. Acta* **1985**, *810*, 338. (b) Kirmaier, C.; Blankenship, R. E.; Holten, D. *Biochim. Biophys. Acta* **1986**, *850*, 275.
(67) Gunner, M. R.; Robertson, D. E.; Dutton, P. L. *J. Phys. Chem.* **1986**, *90*, 3783.
(68) Here it is assumed that the observed absorbance changes around 865 nm for both states $P^+H_A^-$ and $^3P^*$ arise only from the bleaching of P. However, the BPheo anion has a weak absorption in this spectral region. The exact value of the extinction coefficient of H_A^- in the RC is not known. From the difference spectrum of $BPheo^-$/BPheo in solution,[69] it can be

estimated to be 10−15% of the extinction coefficient of P at 865 nm. Indeed, difference spectra of the bleached Q_y-band of P at delay times of 4 and 200 ns, corresponding to $P^+H_A^-$ and $^3P^*$, respectively, have a slightly different shape (data not shown). These differences can be well explained by a spectrally broad absorbance of H_A^- with an extinction coefficient of about 15% of the P ground-state extinction. The additional transient absorbance reduces the bleaching observed for $P^+H_A^-$, so that the concentration of the radical pair relative to $^3P^*$ is underestimated. This leads to an overestimation of Φ_T by at most 15% (relative).

(69) Fajer, J.; Davis, M. S.; Brune, D. C.; Spaulding, L. D.; Borg, D. C.; Forman, A. In *Chlorophyll-Proteins, Reaction Centers, and Photosynthetic Membranes*; Olson, J. M., Hind, G., Eds.; Brookhaven National Laboratory: Upton, NY, 1976; p 74.

(70) Till, U.; Hore, P. J. *Mol. Phys.* **1997**, *90*, 289.

(71) Richter, M. Ph.D. Thesis, Technische Universität München, 1997.

(72) To find the best method for analyzing the nonexponential radical pair recombination data, we performed extensive numerical simulations. Radical pair recombination kinetics were simulated with the semiclassical model, as described in section IV, for a wide range of parameters. The best representation of the kinetics was searched for by fitting these simulation results to various analytical functions.[11] As for the fits of experimental results, simulated data at times shorter than 5 ns were not considered. It was found that monoexponential fits of the overall radical pair decay yield the best results for the radical pair lifetime, $\langle\tau_{RP}\rangle$, averaged over all nuclear spin conformations. The monoexponential time constants obtained from these fits deviate by less than 10% from the true values of $\langle\tau_{RP}\rangle$, which in the semiclassical model can be calculated exactly. Fits to a biexponential or stretched exponential time dependence yield less accurate results for $\langle\tau_{RP}\rangle$ due to the uncertainty with respect to short-lived components which arises from ignoring data for times shorter than 5 ns. For the determination of ΔA_0 and Φ_T, an extrapolation of the measured decay curve to $t = 0$ is needed. It was found that this is carried out most reliably by using a biexponential fit with a fixed amplitude ratio (1/1). When using this method, the error in the determination of ΔA_0 and Φ_T due to the deviations from monoexponentiality is less than 1%.

(73) Lersch, W.; Michel-Beyerle, M. E. *Chem. Phys.* **1983**, *78*, 115.

(74) Ferguson, R. C.; Marquardt, D. W. *J. Chem. Phys.* **1964**, *41*, 2087.

(75) Schulten, K.; Wolynes, P. G. *J. Chem. Phys.* **1978**, *68*, 3292.

(76) McElroy, J. D.; Feher, G.; Mauzerall, D. C. *Biochim. Biophys. Acta* **1972**, *267*, 363.

(77) Okamura, M. Y.; Isaacson, R. A.; Feher, G. *Biochim. Biophys. Acta* **1979**, *546*, 394.

(78) Ogrodnik, A.; Lersch, W.; Michel-Beyerle, M. E.; Deisenhofer, J.; Michel, H. In *Antennas and Reaction Centers of Photosynthetic Bacteria: Structure, Interaction and Dynamics*; Michel-Beyerle, M. E., Ed.; Springer-Verlag: Berlin, 1985; p 198. Here, a factor of 0.5 was erroneously dropped; thus the correct value of the dipole interaction in RCs of *Rb. sphaeroides* is 5.5 G. Due to the similarity of the RCs of *Rb. sphaeroides* and *Cf. aurantiacus*, their structure is expected to be highly similar. Therefore, the dipole interaction should have a similar value for *Cf. aurantiacus*.

(79) Hunter, D. A.; Hoff, A. J.; Hore, P. J. *Chem. Phys. Lett.* **1987**, *134*, 6.

(80) Lang, E. Ph.D. Thesis, Technische Universität München, 1991.

(81) Ogrodnik, A. Ph.D. Thesis, Technische Universität München, 1983.

(82) Lersch, W. Ph.D. Thesis, Technische Universität München, 1987.

(83) Lersch, W. Diploma Thesis, Technische Universität München, 1982.

(84) Boxer, S. G.; Chidsey, C. E. D.; Roelofs, M. G. *Proc. Natl. Acad. Sci. U.S.A.* **1982**, *79*, 4632.

(85) Zysmilich, M. G.; McDermott, A. *J. Am. Chem. Soc.* **1994**, *116*, 8362.

(86) Takiff, L.; Boxer, S. G. *J. Am. Chem. Soc.* **1988**, *110*, 4425.

(87) Shuvalov, V. A.; Parson, W. W. *Proc. Natl. Acad. Sci. U.S.A.* **1981**, *78*, 957.

(88) Hörber, J. K. H.; Göbel, W.; Ogrodnik, A.; Michel-Beyerle, M. E.; Cogdell, R. J. *FEBS Lett.* **1986**, *198*, 273.

(89) Woodbury, N. W.; Parson, W. W.; Gunner, M. R.; Prince, R. C.; Dutton, P. L. *Biochim. Biophys. Acta* **1986**, *851*, 6.

(90) Keupp, W. Ph.D. Thesis, Technische Universität München, 1994.

(91) Here, the effects of rotational depolarization were excluded by considering data after 30 μs only.

(92) Woodbury, N. W.; Parson, W. W. *Biochim. Biophys. Acta* **1984**, *767*, 345.

(93) (a) Ogrodnik, A.; Michel-Beyerle, M. E. In *Photoprocesses in Transition Metal Complexes, Biosystems and Other Molecules. Experiment and Theory*; Kochanski, E., Ed.; Kluwer Academic Publishers: Netherlands, 1992; p 349. (b) Ogrodnik, A. *Mol. Cryst. Liq. Cryst.* **1993**, *230*, 35.

(94) Hartwich, G.; Lossau, H.; Ogrodnik, A.; Michel-Beyerle, M. E. In *The Reaction Center of Photosynthetic Bacteria: Structure and Dynamics*; Michel-Beyerle, M. E., Ed.; Springer-Verlag: Berlin, 1996; p 199.

(95) Holzwarth, A. R.; Müller, M. G. *Biochemistry* **1996**, *35*, 11820.

(96) Haberkorn, R.; Michel-Beyerle, M. E.; Marcus, R. A. *Proc. Natl. Acad. Sci. U.S.A.* **1979**, *76*, 4185.

(97) Michel-Beyerle, M. E.; Ogrodnik, A. In *Progress in Photosynthesis Research*; Baltscheffsky, M., Ed.; Martinus Nijhoff Publishers: Dordrecht, 1990; p 13.

(98) Volk, M.; Häberle, T.; Feick, R.; Ogrodnik, A.; Michel-Beyerle, M. E. *J. Phys. Chem.* **1993**, *97*, 9831.

(99) Bixon, M.; Jortner, J. *J. Phys. Chem.* **1991**, *95*, 1941.

(100) Windsor, M. W.; Menzel, R. *Chem. Phys. Lett.* **1989**, *164*, 143.

(101) Bixon, M.; Jortner, J.; Michel-Beyerle, M. E. In *The Reaction Center of Photosynthetic Bacteria: Structure and Dynamics*; Michel-Beyerle, M. E., Ed.; Springer-Verlag: Berlin, 1996; p 287.

(102) This assumption is supported by the simulations of the nonexponential charge separation described in section VI. If the free energy of $P^+B_A^-$ was significantly higher than assumed here, the nonexponentiality of primary charge separation in RCs of *Cf. aurantiacus* would be expected to be much larger than observed.

(103) Volk, M.; Gilbert, M.; Rousseau, G.; Richter, M.; Ogrodnik, A.; Michel-Beyerle, M. E. *FEBS Lett.* **1993**, *336*, 357.

(104) As can be seen from eq 7, here the logarithm of $k_{ET}T^{1/2}$ has to be plotted versus $1/T$ to obtain E_A.

(105) (a) Frauenfelder, H.; Petsko, G. A.; Tsernoglou, D. *Nature* **1979**, *280*, 558. (b) Frauenfelder, H.; Parak, F.; Young, R. D. *Ann. Rev. Biophys. Biophys. Chem.* **1988**, *17*, 451.

(106) Kleinfeld, D.; Okamura, M. Y.; Feher, G. *Biochemistry* **1984**, *23*, 5780.

(107) Goldstein, R. A.; Boxer, S. G. *Biochim. Biophys. Acta* **1989**, *977*, 78.

(108) Frank, H. A.; Violette, C. A. *Biochim. Biophys. Acta* **1989**, *976*, 222.

(109) Hartwich, G.; Scheer, H.; Aust, V.; Angerhofer, A. *Biochim. Biophys. Acta* **1995**, *1230*, 97.

(110) Frank, H. A.; Chynwat, V.; Posteraro, A.; Hartwich, G.; Simonin, I.; Scheer, H. *Photochem. Photobiol.* **1996**, *64*, 823.

(111) Parson, W. W.; Monger, T. G. *Brookhaven Symp. Biol.* **1976**, *28*, 195.

(112) (a) Schenck, C. C.; Mathis, P.; Lutz, M. *Photochem. Photobiol.* **1984**, *39*, 407. (b) Lous, E. J.; Hoff, A. J. *Biochim. Biophys. Acta* **1989**, *974*, 88.

(113) Hoff, A.J. *Isr. J. Chem.* **1992**, *32*, 426.

(114) Bixon, M.; Jortner, J.; Michel-Beyerle, M. E. In *The Reaction Center of Photosynthetic Bacteria: Structure and Dynamics*; Michel-Beyerle, M. E., Ed.; Springer-Verlag: Berlin, 1996; p 297.

(115) Wang, Z.; Pearlstein, R. M.; Jia, Y.; Fleming, G. R.; Norris, J. R. *Chem. Phys.* **1993**, *176*, 421.

(116) Goldstein, R. A.; Boxer, S. G. *Biophys. J.* **1987**, *51*, 937.

(117) In ref 116 similar distributions were given, using double the width for $f^0(\omega,B)$. This is not correct, as can be seen from a comparison of eq 3 of ref 116 with eqs 6 and 7 in ref 75.

(118) Haberkorn, R. *Chem. Phys.* **1977**, *19*, 165.